NATIONAL ADVISORY COMMITTEE FOR AERONAUTICS

TECHNICAL NOTE 3130

A PROCEDURE FOR THE DESIGN OF AIR-HEATED ICE-PREVENTION

SYSTEMS

By Carr B. Neel

Ames Aeronautical Laboratory
Moffett Field, Calif.

NACA

Washington

June 1954

NATIONAL ADVISORY COMMITTEE FOR AERONAUTICS

TECHNICAL NOTE 3130

A PROCEDURE FOR THE DESIGN OF AIR-HEATED ICE-PREVENTION

SYSTEMS[1]

By Carr B. Neel

SUMMARY

A procedure proposed for use in the design of air-heated systems for the continuous prevention of ice formation on airplane components is set forth. Required heat-transfer and air-pressure-loss equations are presented, and methods of selecting appropriate meteorological conditions for flight over specified geographical areas and for the calculation of water-drop-impingement characteristics are suggested.

In order to facilitate the design, a simple electrical analogue was devised which solves the complex heat-transfer relationships existing in the thermal-system analysis. The analogue is described and an illustration of its application to design is given.

INTRODUCTION

The first designs of aircraft ice-prevention systems utilizing heated air were based on the specification of an arbitrary surface-temperature rise in clear air for the wing and tail surfaces and of an arbitrary heat-flow requirement through the windshield outer surface (e.g., refs. 1, 2, and 3). Subsequently, flight research conducted in natural icing conditions (refs. 4 to 8) provided information enabling a more rational approach to the design problem whereby a system could be designed on a wet-air basis. Along with the research on heat requirements, sufficient data also have been obtained on the meteorology of icing and the rate and area of impingement of water drops on airfoils so that an ice-prevention system can be designed which will provide reasonably adequate protection during flight over arbitrarily selected routes.

This report illustrates a method for the design of ice-prevention equipment in which the components are continuously protected by means of

[1]This report was prepared originally as one of a series of lectures presented at the Airplane Icing Information Course sponsored by the University of Michigan, March 30 - April 3, 1953.

internally circulated heated air. Use is made of existing information
obtained through previous research. In addition, apparatus is described
and demonstrated which should aid materially in the thermodynamic design
of an air-heated system. The heat-transfer and air-flow data presented
in this paper are applicable only at subcritical speeds; however, in gen-
eral, the design procedure delineated herein should be usable at all speeds.

DESIGN PROCEDURE FOR WING AND TAIL SURFACES

Requirements for Adequate Protection
in Icing Conditions

The basic requirement for wing thermal ice-prevention equipment is
that the wing must be maintained sufficiently free of ice accretions to
enable continued safe flight in icing conditions. Some indication of the
amount of ice, either in the form of primary accretions or runback, a wing
can accumulate without deleterious effects is given by the tests reported
in reference 9. Although under certain conditions, some tolerance for ice
formations is shown, the recommended procedure at the present time is to
design for complete evaporation of all impinging water in the most severe
conditions likely to be encountered in a region of continuous icing. A
wing designed on this basis will remain clear of ice under most situations
and will be capable of operation in the most severe conditions likely to
be experienced, with only a relatively small amount of runback forming.
Furthermore, such conditions are encountered only rarely and for short
periods of time.

Establishment of Tentative Heated-Wing Design

Before analysis of a thermal system can be undertaken, a tentative
design must be established. Due to the other requirements associated with
airplane design, there may be little latitude in the thermal-system design,
and the analysis may be resolved into a determination of the required rate
of heated-air flow for a set configuration. Several typical designs of
wing systems and their advantages will be discussed.

The most efficient and generally accepted designs utilize a double-
skin arrangement which directs the heated air across the inner surface of
the wing. Usually, the air is delivered to the double-skin gap through
a spanwise duct formed by the back of the inner skin and a baffle located
several inches behind the wing leading edge. The air enters the gap near
the stagnation line and is directed aft through the double-skin passages.
A number of different inner-skin arrangements have been used, several of
which are shown in figure 1.

Due to the roughness presented to the air in the spanwise duct by the
back surfaces of the corrugated-type passages, it is often desirable to

install a liner against the backs of the corrugations to allow a smoother duct air flow (see fig. 1). In this case, a gap is left either at the rear of the liner or at the leading edge to allow the air to enter the corrugations. When the gap is located at the rear of the liner, the air is forced to flow forward against the portion of the corrugation joined to the outer skin, then aft inside the corrugation. This arrangement provides, in effect, a double-pass heat exchanger, which tends to concentrate the heat in the leading-edge region. A disadvantage of this system is that the flow of heated air is considerably more restricted than if the gap were located at the leading edge, due to the added length and tortuousness of the path. In some designs, it may be necessary, structurally, to retain the wing nose ribs. In this case, a liner to direct the air through the nose-rib openings, similar to the corrugation liner, undoubtedly will be required.

In efficient heated-wing designs, the heating should be concentrated as much as possible in the area of water-drop impingement to obtain evaporation of all intercepted water. Introducing the heated air into the double-skin passages at the leading-edge line of the wing, therefore, is the best arrangement. The use of a liner to aid in concentrating the heat in the leading-edge region, as noted previously, may have some advantage in this regard. In all cases of double-skin construction, there is a conduction of heat from the inner skin to the outer at the points of attachment. Advantage is taken of this conduction in the corrugated-type inner skin, where the area of attachment is large, and is minimized in the case of a dimpled skin, where the area of attachment is small.

The chordwise extent of the double-skin area is determined by the maximum distance of water-drop impingement. Usually, the required percentage-chord coverage will vary from the wing root to the tip.

Selection of Airplane Operating Conditions

The establishment of flight conditions for the design of a thermal ice-prevention system must be made bearing in mind the intended use of the airplane. An airplane intended to be flown at high altitudes, say over mountainous terrain, will have different requirements from one with a relatively low service ceiling. In general, since low-altitude flight is required of all airplanes for approach and landing and high altitude often is critical for an air-heated system, several operating conditions, such as climb, high-altitude cruise, and letdown, should be chosen for analysis to determine the critical condition.

In selecting an airspeed for design, consideration should be given to the effects of speed on the heating requirement. The rate of removal of heat from the outer surface is increased with increase in speed, so

that high speed becomes a critical condition for an air-heated system. Nevertheless, maximum cruising speed should not necessarily be chosen as the design condition. Selection of the design speed should also be guided by the fact that it is common practice for pilots to reduce airspeed when flying through the turbulent conditions which frequently accompany airplane icing.

Selection of Design Meteorological Conditions

Because of a lack of sufficient data, selection of meteorological conditions for design in the past has been somewhat arbitrary. A recent probability analysis of icing conditions (ref. 10), however, provides data from which a designer can choose a wide range of simultaneous combinations of meteorological variables, each having the same probability of being exceeded. Since three variables are involved (liquid-water content, drop size, and air temperature), a three-dimensional plot is obtained which contains an equiprobability surface, such as that shown in figure 2. By use of this equiprobability surface, the most critical combinations of meteorological variables can be established for the thermal system.

As was mentioned previously, conditions representative of the maximum to be encountered in a continuous-icing situation are considered reasonable design criteria. The data presented in reference 10 for layer-type clouds are representative of continuous icing. In selecting design data from reference 10, the designer must choose an exceedance probability, that is, the number of icing encounters which the airplane might be expected to experience in order to exceed the design condition once. Likewise, the anticipated horizontal extent of the icing clouds must also be determined. Suppose, for example, that the airplane is to be operated in the plateau region of the United States (see fig. 3), the system is to be designed for an exceedance probability of 1 in 100 icing encounters, and the horizontal extent of the icing condition is chosen as 50 miles. The equiprobability surface for this situation would appear as shown in figure 4, in which the surface is represented as a two-dimensional plot with constant-temperature contours. The thermal system, then, must provide protection for all combinations of liquid-water content, drop size, and air temperature presented in this figure.

As a means for rapid evaluation of the critical combinations of the meteorological variables, it has been suggested that the exceedance probability for a given component be evaluated considering water-interception rates alone, rather than analyzing the thermal-system performance for all combinations of water content, drop size, and free-air temperature (refs. 10 and 11). Such an approximation is possible in the case of a heated wing because the heating requirement for evaporation of all impinging water depends largely on the amount of water collected. Therefore, by constructing curves of constant weight rate of water-drop impingement on the

equiprobability chart, as illustrated in figure 4, the critical combinations of liquid-water content, drop size, and air temperature are established for the section of wing under consideration. These curves are determined from knowledge of the water-drop trajectories. Each curve of constant rate of interception, then, defines, roughly, the performance of a section of heated wing designed to evaporate all impinging water at a given condition. The critical condition is denoted as the point at which the rate-of-interception curves and the equiprobability curve become tangent. In the example presented in figure 4, the critical icing condition for an air temperature, say, of 20° F is 0.24 gram per cubic meter at 20-microns drop diameter. At this point, the critical rate of water impingement is 4.3 pounds per hour per foot span. Since the probability of encountering high values of water content and, hence, high rates of impingement, is much greater at high air temperatures than at low temperatures, the curves for the higher air temperatures represent the more critical icing conditions for wing systems.

Determination of Rate, Area, and Distribution
of Water-Drop Impingement

Since the rate, area, and distribution of water-drop impingement on the wing have an important influence on the heating requirement, these factors must be evaluated to enable proper thermal-system design. The study of trajectories of water drops approaching various shapes in flight has been the object of a number of investigations (refs. 12 to 28). Most of the procedures developed for the calculation of trajectories are quite laborious and require, in addition to knowledge of the flow field ahead of the airfoil, elaborate computing equipment, such as a differential analyzer. As a result, the cylinder-substitution procedure (ref. 6) has been largely used in the past for the estimation of impingement on airfoils. However, this substitution is inaccurate in many instances (ref. 29), particularly for the case of low-drag airfoils.

Two methods have been developed recently which enable a more accurate determination of the water-drop-impingement characteristics without the need for a differential analyzer or for laborious calculations. The first of these (ref. 16) is by far the simpler procedure, requiring only a knowledge of the airfoil velocity distribution to establish the important impingement parameters. A possible limitation of the method is that it is based on data obtained from fairly thick airfoils (15-percent chord), and there is some question as to its applicability to thin airfoil sections. However, in the absence of definite knowledge of the limitations, this procedure is suggested for computing the water-drop impingement on wing and empennage surfaces, provided, of course, that more exact data are not available for the particular case under consideration. The second of these methods (refs. 15 and 23) requires the construction of some equipment but, once assembled, the apparatus enables the rapid and accurate calculation

of trajectories for any two-dimensional shape. This system appears very attractive for the designer confronted with provision of icing protection for a variety of configurations.

Heat-Transfer Relationships

External heat transfer and evaporation.- During flight in icing conditions, a heated wing is cooled by convection, by evaporation of the water on the surface, and, in the region of water-drop interception, by the water striking the wing. The rate at which heat must be supplied in order to maintain the wing surface at a specified temperature is, therefore, a function of the rates of convection, evaporation, and water impingement. The effect of radiant heat transfer is negligible.

The unit heat loss from a surface exposed to icing conditions and heated above 32° F is expressed by the following equation (all symbols presented herein are defined in Appendix A):

$$q = h_a(t_s - t_d) + h_a(X - 1)K(t_s - t_d) + M_w c_w(t_s - t_w) \qquad (1)$$

in which the expressions on the right-hand side represent the losses due to convection, evaporation, and water impingement, respectively, and where

$$t_d = t_o + \frac{V_o^2}{2gJc_p}\left[1 - \left(\frac{V_l}{V_o}\right)^2(1 - r_f)\right] - 0.622\frac{L_s K}{c_p}\left(\frac{e_d - e_l}{p_l}\right)$$

$$X = 1 + \left(\frac{e_s - e_d}{t_s - t_d}\right)\frac{0.622 \, L_s}{p_l c_p}$$

$$t_w = t_o + \frac{V_o^2}{2gJc_w}$$

The rate of evaporation, or mass transfer, from the heated surface is given as

$$M_{ev} = 0.622 h_a K \left(\frac{e_s - e_l}{p_l c_p} \right) \tag{2}$$

The above equations were taken from reference 30. A simple graphical solution to equations (1) and (2) has been devised in reference 30, enabling quick and accurate calculations to be performed in the analysis of ice-prevention equipment. Equations similar to those shown above, but with a somewhat different arrangement of variables, are given in reference 31, which likewise presents graphical solutions.

In order to solve equations (1) and (2), knowledge of the magnitude of the convective heat-transfer coefficient h_a is required. The most accurate methods for evaluating this coefficient (ref. 32) depend on a determination of the boundary-layer characteristics, a somewhat lengthy procedure. A simplified method sufficiently accurate for design purposes involves the substitution of equations for cylinders and flat plates to approximate the heat-transfer coefficient over a wing (refs. 33 and 34). These equations are as follows:

Leading-edge region

$$h_a = 0.194 \, T_f^{0.49} \left(\frac{V_0 \gamma}{2r} \right)^{0.5} \left[1 - \left(\frac{\varphi}{90} \right)^3 \right] \tag{3}$$

Laminar boundary layer (beyond leading edge)

$$h_a = 0.0562 \, T_f^{0.5} \left(\frac{V_l \gamma}{S} \right)^{0.5} \tag{4}$$

Turbulent boundary layer (beyond leading edge)

$$h_a = 0.51 \, T_f^{0.3} \frac{(V_l \gamma)^{0.8}}{S^{0.2}} \tag{5}$$

In the above equations, γ represents the specific weight of the air at temperature T_f and the prevailing pressure. A graphical presentation permitting rapid evaluation of equations (3), (4), and (5) is contained in reference 30.

The most uncertain factor influencing the convective heat-transfer coefficient is the location of transition from laminar to turbulent flow in the boundary layer and the chordwise extent of the transition region. Disturbance of the boundary layer by the presence of water on the wing surface undoubtedly causes premature transition. Experimental evidence indicates that the start of transition under such conditions occurs near the rear extremity of water-drop impingement (ref. 7). The assumption of the start of transition at this point appears to be a good approximation. At the present time, the extent of the transition region can only be estimated. Based on limited information (refs. 5 and 7), it is suggested that the transition region be assumed to extend chordwise along the surface for a distance roughly equal to three-fourths of the distance from the stagnation point to the start of transition. Although the extent of the transition zone may possibly exceed this value, its use will be conservative. In the transition zone, a linear variation of heat-transfer coefficient with distance may be taken.

A second quantity required in the solution of equations (1) and (2) is the wetness fraction K. In the area of impingement, measurements indicate a value of 1. Aft of the impingement area the water runs back in rivulets, and flight and tunnel data show a rapid decrease from 1 to about 0.3, with a gradual decline in the value of K thereafter. The measured variation in wetness fraction aft of the area of impingement is shown in figure 5, which was taken from reference 35.

Internal heat transfer.- In the transfer of heat from the heated air inside the wing, the outer skin receives heat directly from the air in the double-skin passages and, indirectly by conduction from the inner skin through the joints between the skins. The inner skin is heated by the air in the passages and by the air behind the passages in the leading-edge duct. In cases where a duct liner is installed, the inner skin is heated by conduction through the common joints, and the liner, in turn, receives heat from the air in the duct. If the liner is made of an insulating material, this conduction very likely will be negligible.

The transfer of heat from the air in the double-skin passages of heated-wing systems is unique in that the usual equations for heat transfer from air flowing inside tubes do not apply. Due to severe entrance conditions and curvature of the passages, the air flow apparently is entirely turbulent, and the heat-transfer coefficient is highest at the gap entrance, decreasing to a constant value downstream (refs. 36 and 37). For typical heated-wing designs, the equations derived by Hardy and Morris are considered the most representative. These are

$$\frac{h_{a_p} L}{k} = 0.152 \left(\frac{GL}{\mu}\right)^{0.7} \tag{6}$$

for the entrance region, and

$$\frac{h_{a_p} d_h}{k} = 0.025 \left(\frac{G d_h}{\mu}\right)^{0.8} \tag{7}$$

beyond the entrance region when steady pipe flow has been established. The entrance length extends for 25 hydraulic diameters from the entry to the passages and, in this region, equation (6) applies. Beyond this point, the value of h_{a_p} is constant and can be computed by use of equation (7). Equations (6) and (7) were determined empirically from tests of a corrugated double-skin arrangement (ref. 36). It is suggested that, when a duct liner is employed with the air-entrance gap located at the rear of the liner (fig. 1(b)), the entrance length for equation (6) be measured from this point.

Measurements of the heat conduction through the joints of double-skin assemblies are comparatively few. References 36 and 38 contain results of measurements of the thermal resistances of typical double-skin joints. Reference 38, in particular, gives thermal-resistance values for five different assembly procedures, encompassing riveting, cementing, and spot welding. Results of more general investigations of the resistances of joints are presented in references 39 and 40. The measurements reported in references 36 and 38 are in good agreement, and the values given in these two reports are considered the most representative presently available. When a leading-edge-duct liner is used, these data may also be applied in the calculation of heat flow from the liner to the inner skin.

An analysis of the data of reference 36, which presents limited measurements of the transfer of heat from the air in the leading-edge duct behind corrugated double-skin passages to the inner skin in the absence of a liner, indicates that the following equation applies:

$$\frac{h_{a_d} d_h}{k} = 0.30 \left(\frac{G d_h}{\mu}\right)^{0.6} \tag{8}$$

wherein the term d_h represents the hydraulic diameter of the leading-edge duct.

In the case of a smooth inner skin utilizing spacer strips (fig. 1(a)) or, in the case of a duct liner, the value of h_{a_d} may be determined from the equation for turbulent pipe flow, as suggested in reference 5:

$$\frac{h_{a_d}d_h}{k} = 0.02 \left(\frac{Gd_h}{\mu}\right)^{0.8} \tag{9}$$

Heated-Air Pressure Losses

Pressure loss in the double-skin passages.- As in the case of heat transfer in the double-skin passages, the usual methods for calculating pressure losses are not applicable. The effects of curvature and entrance condition apparently cause higher pressure losses than predicted. The data considered the most representative for heated-wing systems showed no difference in the pressure-drop measurements for isothermal or nonisothermal flow (ref. 37). In evaluating these data to obtain a generalized relationship, the conventional equation involving entrance head loss and friction loss was employed:

$$\Delta P = \frac{G^2 v_{av}}{2g} \left(N + \frac{fL}{d_h}\right) \tag{10}$$

where N is the entrance coefficient and f is the friction factor. Figure 6 presents values of friction factor as a function of Reynolds number, as computed from the data of reference 37 using the suggested value of 0.75 for N. Although these data were obtained with one specific type of double skin (corrugated), it is proposed that pressure losses for other types of double skin be computed from equation (10), using $N = 0.75$ and values of f from figure 6.

It will be noted that the pressure loss in equation (10) and in subsequent equations is given in terms of the hydraulic diameter rather than the hydraulic radius, as used in reference 41; hence, the friction factors presented in this report are four times those appearing in reference 41.

Pressure loss in the leading-edge duct.- The pressure drop of the air flow in the leading-edge duct may be calculated from equation (22c), page 128 of reference 41, or

$$\Delta P = \frac{G^2 \Delta v}{g} + \frac{fLG^2 v_{av}}{2gd_h} \qquad (11a)$$

where Δv represents the change in specific volume of the air in the section of duct under consideration. In most cases, Δv is negligible and equation (11a) reduces to

$$\Delta P = \frac{fLG^2 v_{av}}{2gd_h} \qquad (11b)$$

For smooth ducts, such as would exist in designs using a smooth inner skin or duct liner, the value of the friction factor f is given by

$$f = \frac{0.184}{(Gd_h/\mu)^{0.2}} \qquad (12)$$

which is a form of equation (9a), page 119, reference 41. When a corrugated-type inner skin is used without a liner, the value of f for the duct may be approximated from

$$f = \frac{0.22}{(Gd_h/\mu)^{0.2}} \qquad (13)$$

which is representative of the data obtained for flow in rough pipes. (fig. 51, p. 118, ref. 41).

Calculation of Required Rate of Heated-Air Flow

The calculation of the heated-air-flow rate through the double-skin passages necessary to evaporate all impinging water under the critical design condition requires the solution of a very complex heat balance. The rate of evaporation and dissipation of heat from the outer surface is a function of the surface temperature, which, in turn, is a function of the heated-air-flow rate and temperature. The temperature of the air at any point in the double skin depends on the amount of heat previously removed from the air. In addition, conduction of heat from the inner to the outer skin and chordwise along the skins complicates the picture even further.

One method used previously in thermal-system analyses (refs. 42 and 43) utilizes the simplifications of assuming a constant surface temperature throughout the heated area and neglecting heat conduction. The heated-air-flow rate required to deliver the resulting quantity of heat is then computed. This procedure has the disadvantage that errors of an unknown magnitude are introduced, due to the fact that the actual surface temperature rarely is uniform and heat conduction in the double-skin system can have an important influence on surface temperature. A more accurate method for calculating the required air-flow rate is to divide the double skin chordwise into several segments and analyze the system by use of a step-by-step trial-and-error procedure (ref. 3). A heat balance is obtained for each segment in sequence as the passage of the air through the double-skin gap is analyzed. Such a procedure is extremely laborious, especially in view of the fact that in a heated-wing analysis involving variable surface temperature, the effective coefficient of external heat transfer varies with the assumed surface temperature. In addition, both upper and lower surfaces of the wing at several spanwise stations must be analyzed to establish the required heated-air-flow distribution.

In order to facilitate the calculation of required flow rate, the use of an electrical-analogue system to simulate the flow of heated air in the wing can aid considerably. In utilizing the electrical analogy, an electric model is assembled to represent a portion of a wing heated internally with air. Such a model was constructed and used to illustrate the analysis of a hypothetical air-heated wing. The model, which is shown in figure 7, consists of an arrangement of electrical resistances and capacitances connected in such a manner as to simulate a thermal circuit. In the electrical circuit, electrical resistance and capacitance represent thermal resistance and capacitance, current flow represents heat flow, and voltage difference represents temperature difference. The resistances of the analogue network consist of rheostats and fixed resistors, whereas the capacitances consist of condensers. A rotating commutator and slip-ring assembly is employed to switch the condensers through the circuit to simulate the travel of heated air through the double-skin passages. Each condenser receives an electrical charge immediately before it is switched into the circuit. This represents the initial heat energy contained in the air before its entry into the double-skin gap. As the condenser is switched through the circuit, part of its charge is lost, representing the loss of heat of that portion of the air and its corresponding decrease in temperature. A microammeter is used to measure the current flow at various locations. This provides a measure of the heat flows and temperatures. A simplified circuit diagram illustrating a portion of the analogue system is presented in figure 8. The theory of the electrical analogy is discussed briefly in Appendix B.

The electrical-analogue arrangement permits rapid determination of the required air-flow rates. It automatically takes into consideration such complex effects as air-temperature drop and heat conduction within

the double-skin system. A certain amount of trial-and-error procedure is still required, but, nevertheless, the answer is quickly established.

Two basic steps are required in this trial-and-error procedure. These are (1) to obtain the surface-temperature distribution for an assumed heated-air-flow rate, and (2) to compute the total rate of evaporation of water for this temperature distribution. If the total rate of evaporation does not equal the rate of impingement, the procedure must be repeated for different air-flow rates until the calculated rate of evaporation is made to equal the rate of impingement. When the required flow rates have been determined for both upper and lower surfaces at several spanwise stations, the pressure losses must be calculated for the double-skin passages and the leading-edge duct to assure that a pressure balance has been attained. Very often a pressure balance will not be achieved such that an ideal flow distribution will result. In such cases, portions of the wing will either be overheated or underheated. If these conditions are intolerable, it may be necessary to investigate a different double-skin arrangement. In any case, employing an electrical-analogue system will facilitate the heated-wing analysis. An example illustrating the application of the electric model to such an analysis is given in Appendix C.

Discussion of the Use of an Electric Model
in Heated-Wing Design

The utilization of an electrical analogue in the design of air-heated wing systems for ice prevention has two important advantages over previous methods of analysis. First, it enables the rapid determination of the correct heated-air-flow rate for any chosen double-skin configuration. Such an application of the analogue technique is demonstrated in Appendix C. Second, due to the versatility of the analogue, its use permits easy variation of configurations and conditions to guide the designer in improving the efficiency of the thermal system. Two specific examples of this will be cited.

In calculating the analogue resistances representative of the corrugated double-skin arrangement considered in the example of Appendix C, it was noted that a fair degree of insulation, in effect, exists between the inner and outer skins of a typical corrugated-passage design, even though the skins have been riveted together. As a result, tests were performed in which the thermal resistance of the joints was decreased to zero, a situation which might be approached in practice by seam-welding the skins together. It was found that, for the particular cases considered, the flow rate of heated air could be reduced from 10.0 to 7.3 pounds per hour per passage at the wing-root station, and from 10.8 to 7.7 pounds per hour per passage at the wing-tip station, all other conditions constant. This represents decreases in the heat requirement of 27 and 29 percent.

Such a revision obviously increases the thermal efficiency of the double-skin system. This is exemplified in the curves of chordwise surface-temperature distribution shown in figure 9 for the two stations at the two joint conditions. It is seen that with the increased heat transfer resulting from the improved thermal bond between skins, a higher surface temperature was obtained in the leading-edge region, even with lower air-flow rates, allowing lower surface temperatures to exist in the after portion. This provides a higher thermal efficiency since the heat is more concentrated in the area of impingement where the surface is entirely wetted and, consequently, the evaporation rates are highest.

Incidentally, the curves of figure 9 show how far from uniform the surface temperature of a heated wing is apt to be, and it is apparent that methods of analysis which assume a constant temperature may lead to error.

A second possible means of decreasing the heat requirement was investigated using the electric model. It becomes evident in the performance of an analysis of a wing thermal system that a considerable amount of heat is wasted in the heated region aft of the area of impingement, where the water runs back in rivulets, and only a small portion of the heat delivered is utilized for evaporation. This is illustrated in figure 10, which shows the distribution of evaporation rate for the wing-root station analyzed previously. Most of the water is evaporated in the region of impingement, even though this area is only three-eighths of the total heated area. It may be reasoned that if the wing surface were treated with a wetting agent which would decrease the surface tension of the water sufficiently to allow it to run back as a sheet, rather than in rivulets, the heat in this region would be utilized much more effectively. A test was conducted, therefore, to determine the magnitude of possible thermal saving under such a condition. For the particular case of the wing-root station, the required heated-air-flow rate could be reduced from 10.0 to 6.6 pounds per hour per corrugation, representing a reduction of 34 percent, if the water aft of the impingement area were made to cover the surface completely. The distribution of evaporation rate would then appear as the dashed line in figure 10. Due to the increased evaporation rate now made possible in the area aft of the impingement limit, it is no longer necessary to concentrate the heat in the region of impingement, and the surface temperature for the entire heated area may be reduced as indicated in figure 11.

It should be noted that the magnitude of the reductions in heat requirement cited for these two examples apply specifically only to the cases considered. This is particularly true in the latter example, where the possible decrease in heat requirement is dependent upon the ratio of area of impingement to total heated area. It is probable, however, that similar reductions could be obtained for other cases of wing ice-prevention systems.

A somewhat discouraging fact that becomes evident when analyzing wing ice-prevention equipment is that even for low values of liquid-water

content, very high heated-air-flow rates will be required at high speeds, unless improvements are made to currently employed systems. This, of course, is the reason why considerable interest has been shown in wing cyclic de-icing systems, wherein reductions in heating requirements can be achieved. However, by increasing the thermal efficiency through improvements in both the internal heat-transfer processes and the external evaporative processes, it appears that heating requirements can be reduced to the point where continuous air-heated ice-prevention systems, with their attendant aerodynamic advantages over cyclic systems, may be practical for high-speed aircraft. In this regard, the use of an electric model, as suggested before, can aid materially. Not only can it help the designer to obtain the most efficient operation from existing configurations, but it also can aid in guiding research directed toward increasing thermal-system efficiency.

A desirable feature of the electric model is that it is relatively inexpensive to construct. On the basis of the experience gained through construction of the experimental model described herein, it is believed that an analogue of this type suitable for analysis of a variety of air-heated components could be built for only a few thousand dollars. It appears quite reasonable, therefore, to construct an electric model for the specific purpose of designing an air-heated ice-prevention system.

DESIGN PROCEDURE FOR WINDSHIELDS

In this section, the criteria and equations required in the design of an air-heated windshield will be considered. The windshield system assumed for discussion will be the conventional double-panel arrangement consisting of two panels separated by a small gap through which the heated air circulates.

Requirements for Adequate Protection
in Icing Conditions

The basic requirement for a windshield ice-prevention system is that the windshield be maintained sufficiently clear to allow adequate visibility. To maintain a windshield free of ice accretions, it is necessary only to raise the temperature of the surface slightly above freezing, rather than to evaporate all impinging water, as in the case of wing ice prevention. The formation of runback ice accumulations from the windshield area is not considered sufficiently serious aerodynamically to warrant the excessive heating loads which would result by attempting to evaporate all intercepted water.

Selection of Design Meteorological Conditions

The most severe icing conditions from the standpoint of windshield ice prevention are those occurring at low air temperatures (ref. 8). Therefore, a selection of design meteorological conditions should be guided by this fact. An obviously important consideration in this selection is that only those conditions under which ice will form on the windshield should be investigated, inasmuch as it has been shown that windshield ice will not form when the water-drop size is small. In general, then, critical meteorological conditions will consist of large drop sizes at low air temperatures.

As in the selection of design meteorological conditions for the wing system, it is suggested that the data of reference 10 be used in the determination of the critical icing condition for the windshield. In this regard, curves of constant rate of water interception superimposed on the equiprobability charts of reference 10 should prove useful in selecting the design condition.

Determination of Rate, Area, and Distribution
of Water-Drop Impingement

In the absence of exact knowledge of the water-drop impingement characteristics for a particular windshield configuration, a substitution procedure can be employed (ref. 8). This procedure involves the substitution of generalized shapes, for which water-drop trajectories have been calculated, for the various windshield configurations. The shapes most applicable in this regard are ribbons and spheres, for which trajectory data are presented in reference 12. The particular object substituted depends on the type of windshield to be protected. For flat-plate and V-type windshields, the assumption is made that the rate of impingement on the windshield panel is equal to the rate of impingement on the projected area of the panel considered as one-half a ribbon (see fig. 12(a)).

In the case of a windshield flush with the fuselage contour, it is assumed that the impingement would be the same as that on the windshield area projected onto a sphere having a diameter equal to the maximum diameter of the fuselage. This is illustrated in figure 12(b). The unit rate of water interception, then, may be approximated from the formula developed in reference 8.

$$M_W = 0.112 \frac{E_M V_o m}{1 - \cos \theta_M} \tag{14}$$

where the terms E_M and θ_M, the collection efficiency and angle of impinge-
ment for the sphere, respectively, are computed from the data of refer-
ence 12.

Heat-Transfer and Air-Pressure-Loss Relationships

External heat transfer.- The same heat-transfer processes discussed
previously for the case of a heated wing in icing conditions apply to a
heated windshield. Thus, the heat flow is defined in equation (1), which
can be readily solved by use of the chart of reference 30.

For the case of a windshield panel, the convective heat-transfer coef-
ficient, as suggested in reference 8, may be calculated from equation (5),
where S is measured from the leading edge of the panel for flat-plate
and V-type windshields, and from the fuselage nose in the case of flush
windshields.

The value of the wetness fraction K should be taken as 1 for wind-
shield calculations.

Internal heat transfer.- The internal heat-transfer process for wind-
shields is greatly simplified over that for wings in that the outer panel
is heated only by the air in the double-panel gap and receives no heat by
conduction, as in wing double-skin arrangements. The equation for deter-
mining the internal heat-transfer coefficient is the turbulent-pipe-flow
formula introduced earlier as equation (9). This equation has been found
to be applicable to the flow of air in rectangular ducts of large aspect
ratio (p. 198, ref. 41).

Heated-air pressure loss.- The pressure loss of the air passing
through the windshield gap is given by the previously presented equation,
(11a). Values of the friction factor f may be computed from equa-
tion (12).

Calculation of Required Rate of Heated-Air Flow

In order to simplify the analysis, air-heated windshield systems in
the past generally have been analyzed on the basis of an assumed uniform
surface temperature. A more accurate solution will result by considering
the variation of conditions for the entire surface, and by determining
the required heated-air-flow rate accordingly. In this connection, the
application of an electric model, such as that described for wing-system
design, to the analysis of air-heated windshields will greatly facilitate
the design calculations. The same general procedure may be followed; that

is, to divide the double-panel system into a number of segments and to determine the air-flow rate required to maintain all points on the outer surface above freezing temperature.

Discussion of Limitations Influencing
Air-Heated Windshield Systems

Heated-air systems for windshield ice prevention may not prove practical for high-speed aircraft. Certain design considerations impose limitations which very likely could make excessively high air-flow rates required. For example, the strength of most windshield materials is reduced at temperatures above about 250° F, and for this reason the inlet temperature of the circulating air will be limited. The probability of large thermal stresses in the glass resulting from high air temperatures is another reason for limiting the air temperature. By so limiting the air temperature, small gap sizes or high air-flow rates will be necessary to obtain the required heat transfer, and the attendant air-pressure drop may be of such magnitude that a blower will be required. The use of thick windshield panels in military aircraft further aggravates the situation. Therefore, unless other factors make air-heating of windshields more attractive, the use of electrical heating may prove to be more feasible for windshield ice prevention of high-speed airplanes.

DESIGN PROCEDURE FOR RADOMES

Requirements for Adequate Protection
in Icing Conditions

Protection of radomes against icing requires that the surface be maintained sufficiently clear to enable successful transmission of the radar signal. Whether or not complete evaporation of all impinging water is necessary will depend on the undesirability of runback ice accretions aft of the radome and on the tolerance of the radar system for water running on the radome surface. Some measurements of the attenuation of the radar signal as a result of water on the radome surface are presented in reference 44.

Proposed Heating Arrangement

In the following discussion, the radome will be assumed to constitute the forward portion of the airplane nose. Consideration will be given only to the thermal-system aspect of radome design although, in an actual case, attention must also be given to the effects of the thermal-system

design on the transmission of electrical energy. The heating system proposed for consideration will be a double-skin arrangement formed by the outer housing and an inner shell, which are separated by the circulating-air gap, as illustrated in figure 13. In this figure, the heated air is shown as entering the gap at the forward end of the radome and exhausting at the rear. This could be accomplished most easily by introducing the heated air into the radar antenna chamber, but such an arrangement may be impracticable due to possible temperature limitations of the radar equipment. If this is the case, reversal of the air-flow direction may be necessary, although this scheme probably would provide a less efficient ice-prevention system.

Determination of Rate and Area of
Water-Drop Impingement

As in the case of windshields, probably the most expedient method for determining the impingement characteristics on radomes is to utilize a substitution procedure, in the event that more exact information is not available. The method proposed is to assume that the impingement on the radome would be the same as that on a sphere with a radius equal to the nose radius of the radome. The data of reference 12 can be used to compute the rate and area of water interception on the sphere. Experimental results have shown the sphere-substitution procedure to provide a good approximation (ref. 44). Calculated impingement data for various radome shapes, which may be of aid in determining water-drop impingement characteristics, are given in references 45 to 48.

Heat-Transfer and Air-Pressure-Loss Relationships

External heat transfer.- The external heat transfer can be calculated by use of equation (1). Values of the convective heat-transfer coefficient may be computed by the method developed in reference 49 for streamline bodies. Experimental data on the convective transfer of heat from an ellipsoid and from spheres, which should prove useful in establishing values of heat-transfer coefficient, are presented in references 50 and 51, respectively. It is suggested that the position and extent of transition from laminar to turbulent flow be taken as proposed previously for wing-system analysis. The wetness fraction K may also be taken as discussed for wings.

Reference 46 gives a thorough treatment of the heating requirements for icing protection of radomes, and should be helpful in the design of radome heating systems. An additional study of the external heat requirements for radomes is contained in reference 52.

Internal heat transfer.- The heat-transfer relationship considered representative of the internal-flow conditions is given in equation (9), which was also suggested for air-heated windshields.

Heated-air pressure loss.- The pressure loss of the air passing through the double-skin gap may be computed from equation (11a), with values of the friction factor obtained from equation (12).

Calculation of Required Rate of Heated-Air Flow

The procedure outlined for wings and windshields in the foregoing sections can also be utilized for radomes to determine the required air-flow rate for ice prevention. As before, an electric model can provide a rapid solution to this problem. In applying the electric model, division of the radome heating system for computing equivalent electrical values must be made in such a manner as to provide equal volumes of heated air between two arbitrarily selected streamlines for all segments, as indicated in figure 13. This is necessary to retain the air-flow analogy.

COMMENTS ON THE DESIGN OF OTHER COMPONENTS
OF THE THERMAL SYSTEM

The remainder of this report will be devoted to a brief discussion of the design of other components of the thermal system. Detailed design data will not be presented inasmuch as this would entail an excessive discourse to treat all situations fully, and such information is adequately covered in available publications.

Propellers

Basically, the procedure for designing an air-heated propeller is the same as that for a wing. The external heat-transfer equations presented for a wing apply equally to the propeller. Internally, the situation is somewhat different in that the heated-air-flow direction in accepted designs is spanwise from the root to the tip of the propeller. The external and internal heat-transfer processes, including analytical and experimental studies to obtain improved internal heat transfer, are treated extensively in references 53 to 58.

The thermal requirements for a propeller should be based on maintaining the heated area just above freezing temperature, rather than on evaporating all intercepted water, as in the case of a wing. Evaporation of all impinging water would impose exorbitant heating loads on the system,

and propeller efficiency losses resulting from runback ice accretions undoubtedly would be quite small (ref. 59).

In the analysis and design of an air-heated propeller, the application of an electrical-analogue system should prove extremely effective, since the blade metal is comparatively thick and, with the addition of internal fins, the heat-conduction effects, which are easily represented electrically, become very important.

Air Inlets and Scoops

Air inlets and scoops which are heated internally by air can be designed in much the same manner as heated wings. One possible exception to the procedure is that it may not be required that all impinging water be evaporated. This is a choice that should be determined on the basis of any adverse effects which might result from runback ice formations. Again, an electric model can be useful in the design.

Air Ducts

The primary concern with the heated-air distribution ducts is that they transport the air with a minimum of thermal and pressure losses. This requires good insulation and clean aerodynamic design. Several papers (refs. 60 to 64) have been written on the aerodynamic design of ducts. The air flow in ducts with sharp bends near the entrance region may become obstructed by the deposit of ice. Some information in this regard may be found in reference 65.

With the advent of cabin pressurization, a new strength-requirement problem has arisen in the design of air ducts. Collapsing of ducts located in pressurized areas can readily occur if attention has not been given to the reduction in strength of the duct material at elevated temperatures, nor to possible column failure of the duct resulting from insufficient end clearance for thermal expansion.

Heat Exchangers

The design of suitable heat exchangers of adequate capacity is a specialized field in itself. Many tests have been performed and many reports have been written on this subject. A few of the more pertinent of these works will be cited. Reference 34 probably contains the most complete information on the design of aircraft exhaust gas and air heat exchangers available at the present time. A good bibliography pertaining

to heat-exchanger design is also presented therein. An illustration of the design of a heat exchanger which was actually installed in an airplane thermal ice-prevention system is given in reference 66. The effect of altitude on the output of an exhaust-gas-and-air heat exchanger is discussed in reference 5. The calculation of pressure losses in heat-exchanger systems is covered in references 67 and 68, and this subject is also considered in the analysis of reference 66.

Ames Aeronautical Laboratory
      National Advisory Committee for Aeronautics
            Moffett Field, Calif., Jan. 20, 1954

APPENDIX A

SYMBOLS

A area perpendicular to direction of heat flow, ft^2

A_p cross-sectional area of air duct or passage, ft^2

C electrical capacitance, farads or microfarads

c_p specific heat of air at constant pressure, Btu/lb, ^oF

c_w specific heat of water, 1 Btu/lb, ^oF

d_h hydraulic diameter of air duct or passage, $\dfrac{4A_p}{\text{perimeter}}$, ft

E electrical potential, volts

E_M water-drop-collection efficiency, dimensionless

e saturated water-vapor pressure at corresponding temperature, in. Hg

f friction factor for air flow in duct or passage, dimensionless

G weight-rate of air flow per unit of cross-sectional area, lb/sec, ft^2

g acceleration due to gravity, 32.2 ft/sec^2

H effective coefficient of total heat transfer, Btu/hr, ft^2, ^oF

h convective heat-transfer coefficient, Btu/hr, ft^2, ^oF

I electrical current flow, amperes or microamperes

J mechanical equivalent of heat, 778 ft-lb/Btu

K surface-wetness fraction, dimensionless

k thermal conductivity, Btu/hr, ft^2, $^oF/ft$

k_j conduction coefficient of joints, Btu/hr, ft^2, ^oF

L length or distance, ft

L_s latent heat of evaporation of water, Btu/lb

M_{ev} rate of evaporation of water per unit of surface area, lb/hr, ft^2

M_{ev_T} total rate of evaporation of water, lb/hr, ft span

M_T total rate of interception of water, lb/hr, ft span

M_w rate of interception of water per unit of surface area, lb/hr, ft^2

m   liquid-water content of ambient air, grams/meter^3

N   entrance pressure-loss coefficient, dimensionless

n   number of commutator segments in electric model

ΔP air-pressure loss, lb/ft^2

p   absolute static pressure, in. Hg

q   rate of heat transfer per unit of surface area, Btu/hr, ft^2

R   electrical resistance, ohms or megohms

r   leading-edge radius of airfoil, ft

r_f temperature-recovery factor, dimensionless

S   surface distance from stagnation point in stream direction, ft

T   absolute temperature, $^\circ$R

T_f arithmetic average of temperature of heated surface and free-stream
            air temperature, $^\circ$R

t   temperature, $^\circ$F

V   air velocity, ft/sec

v   specific volume of air, ft^3/lb

W   weight, lb

w   weight-rate of air flow per passage, lb/hr

X   Hardy's evaporation factor, dimensionless

γ specific weight, lb/ft^3

θ_M central angle, measured from stagnation point to farthest point of impingement on the surface of a sphere, deg

μ viscosity of air, lb/sec, ft

φ central angle measured from stagnation point of airfoil-leading-edge cylinder, deg

ω commutator rotational speed, rpm

Subscripts

Except where otherwise defined, the following subscripts apply:

a external air

a_d air in wing leading-edge duct

a_p air in double-skin passage

av average

d heat-transfer datum

l local

o undisturbed free stream

s surface

w water

APPENDIX B

THEORY OF ELECTRICAL ANALOGY FOR THE SIMULATION OF HEAT

FLOW, PRACTICAL DESIGN CONSIDERATIONS FOR AN ANALOGUE,

AND A COMPARISON OF CALCULATED AND MEASURED RESULTS

USING AN ELECTRIC MODEL

Theory of Electrical Analogy

General heat-flow analogy.- The flow of heat by conduction and con-
vection is analogous to the flow of electricity through an electrical
resistance. The rate of heat flow varies with the thermal resistance and
temperature gradient, whereas electrical current flow varies with the elec-
trical resistance and voltage difference. In both cases the variations
are identical. Likewise, the variation of heat flow with time from a
thermal mass is identical to the current-flow variation with time from an
electrical capacitance. Therefore, by substitution of an electrical cir-
cuit for its corresponding thermal circuit, heat-flow studies can be made
by comparatively simple electrical measurements. Great flexibility is
achieved through the ease with which values of the electrical counterparts
can be varied to investigate different thermal effects. The primary use
of the electrical analogy is in the study of transient heat-flow problems
where thermal capacitance as well as thermal resistance is of importance.

In the electrical analogy, the following equivalent relationships
apply:

Thermal	Electrical
1 Btu	1 coulomb
1 Btu/sec	1 coul./sec = 1 ampere
1 $^{\circ}$F	1 volt
1 $^{\circ}$F sec/Btu	1 volt sec/coul. = 1 ohm
1 Btu/$^{\circ}$F	1 coul./volt = 1 farad

In use, the values of electrical resistance and capacitance take the form

$$R = \frac{3600 \ L}{kA} \tag{15a}$$

for conduction, or

$$R = \frac{3600}{HA} \qquad (15b)$$

for convection, or convection plus evaporation, and

$$C = (Vol) \gamma c_p \qquad (16)$$

where

A   area perpendicular to direction of heat flow, ft^2

c_p specific heat, Btu/lb, $^\circ F$

C   electrical capacitance, farads

H   effective heat-transfer coefficient, Btu/hr, ft^2, $^\circ F$

k   thermal conductivity, Btu/hr, ft^2, $^\circ F/ft$

L   distance in direction of heat flow, ft

R   electrical resistance, ohms

Vol   volume, ft^3

γ specific weight, lb/ft^3

Heated-air-flow analogy.- In the specific application of an electrical-analogue system to the flow of heated air under steady-state conditions, the term C represents the heat capacity of the air and R, the various thermal resistances. For this application, the velocity of the air must be considered in addition to resistance and capacitance, since the amount of heat removed from the air in a given distance of travel is governed by the time required for its passage over that distance. In this case,

$$RC \frac{V a_p}{\Delta L} = constant \qquad (17a)$$

The above relationship controls the selection of values such that the condensers in the analogue system will lose their charge proportional to the

heat loss of the air as it progresses through the passage. Equation (17a) is derived in the following manner. In a short length of air passage, the thermal energy loss of the air can be equated to the heat transferred to the adjacent surface, or

$$wc_p \Delta t_{a_p} = hA_s(t_{a_p} - t_s)$$

where Δt_{a_p} represents the temperature drop of the air. This equation may be rearranged to give

$$\frac{wc_p}{hA_s} = \frac{t_{a_p} - t_s}{\Delta t_{a_p}}$$

Both sides of this equation equal a dimensionless constant. Therefore, substitution of equivalent electrical terms for the thermal terms may be made without altering the constant. Considering the left side of the equation, if the length of air passage is ΔL feet containing (Vol) cubic feet, and the air velocity is V_{a_p}, w can be expressed as $3600 \dfrac{(\text{Vol})\gamma V_{a_p}}{\Delta L}$, and

$$\frac{wc_p}{hA_s} = 3600 \frac{(\text{Vol})\gamma c_p V_{a_p}}{hA_s \Delta L} = \text{constant}$$

Then, since $h = H$ in the case of convection, substitution of equations (15b) and (16) into the above relationship yields equation (17a).

When an electric model is used employing a commutator arrangement, such as that used for the tests described herein (see fig. 7), the commutator rotational speed may be substituted for the term $\dfrac{V_{a_p}}{\Delta L}$ in equation (17a), or

$$RC\omega = \text{constant} \tag{17b}$$

where

$$\omega = \frac{60 \, V_{a_p}}{n \Delta L} \tag{18a}$$

In the above equation n represents the number of commutator segments and $\triangle L$ the distance of travel of heated air during the passage of one segment past a brush. The value of V_{a_p} may be expressed as

$$V_{a_p} = \frac{wv_{av}}{3600A_p}$$

and equation (18a) becomes

$$\omega = \frac{wv_{av}}{60A_p n \triangle L} \tag{18b}$$

The value of C represents the thermal capacity of the volume of air present in a segment of air passage $\triangle L$ feet long. If $\triangle W$ represents the weight of air in the segment, then

$$C = \triangle W c_p \quad \text{farads}$$

or

$$C = \triangle W c_p \times 10^6 \quad \text{microfarads}$$

Since

$$\triangle W = \frac{\triangle L A_p}{v_{av}}$$

then

$$C = \frac{\triangle L A_p c_p}{v_{av}} \times 10^6 \quad \text{microfarads} \tag{19}$$

If equations (18b) and (19) are combined,

$$C\omega = \frac{c_p W}{60n} \times 10^6 \qquad\qquad (20)$$

where C is in microfarads.

When the above equations are applied to the calculation of values for an electric model, values of R are computed using equations (15a) and (15b), and values of Cω are determined from equation (20). The values of R, C, and ω may then be adjusted for convenience, provided equation (17b) is satisfied. If the values of R or C are to be adjusted, all values of R or C in the network must be changed proportionately. For instance, if it is desired to increase a resistance value by a factor of 10, all resistances in the circuit must be increased by the same factor.

Conversion of measurements.- Temperature differences are directly proportional to voltage differences in the analogue system, and heat flow is likewise directly proportional to current flow. Since temperature difference and heat flow are directly related by the equations

$$q = H\triangle t$$

and

$$q = \frac{k}{L}\triangle t$$

or electrically,

$$I = \frac{E}{R}$$

then the value of temperature difference may be obtained indirectly by the measurement of heat flow. The converse also is true. In the electrical analogy, then, a measure of temperature difference is obtained from measurements of current flow through known resistances. To convert the electrical measurements directly in terms of thermal units, a known electrical value must be assigned a specific thermal value. For example, a potential difference of 25 volts may be considered to represent a temperature difference of 100° F. Then an actual measurement of 10 volts is equivalent to a 40° F temperature difference.

In the case of the application of the electric model, the voltage of the battery which precharges each condenser prior to its entry into the analogue circuit may be considered to represent the temperature rise above

ambient of the heated air in the leading-edge duct at the entrance to the
double-skin passages. The surface-temperature rise, then, is obtained by
determining the voltage across the external-air resistance. The equation
expressing this relationship is

$$\frac{\Delta t_s}{\Delta t_{a_d}} = \frac{E_s}{E_{a_d}}$$

where the subscript s denotes the surface condition and a_d pertains
to the initial heated-air condition at the passage entrance. Since cur-
rent, rather than voltage, measurements are made with the electric model,
this equation becomes

$$\Delta t_s = \Delta t_{a_d} \frac{I_s R_a}{I_{a_d} R_{a_d}} \tag{21}$$

where R_a is the external-air resistance. The value of R_{a_d} is chosen
arbitrarily, and I_{a_d} is the measured current flow through R_{a_d} when the
battery voltage E_{a_d} is impressed across this resistance.

Practical Considerations Regarding the Design
and Use of an Electrical Analogue

A few of the more pertinent aspects concerning the design and use of
an electrical analogue are worthy of note at this point. A more detailed
discussion of the requirements associated with the design of electrical-
analogue systems is contained in reference 69. Further information is
also given in reference 70, which presents a comprehensive consideration
of the design of analogues for steady-state applications requiring only
electrical-resistance elements.

Requirements for condensers.- The leakage resistance of the conden-
sers used to simulate thermal capacity in the electrical network should
be at least of the order of 100 times the effective resistance of the
circuit in which they are connected. Since analogue-circuit resistances
generally are several megohms, this means that the leakage resistance
must be very high, and for most applications electrolytic condensers will
be unsatisfactory. Most commercially available paper, mica, and oil-filled
condensers, on the other hand, have been found to possess suitable leakage-
resistance characteristics. Resistance values above 1000 megohms can be
expected for condensers of these types with nominal capacitance ratings
up to 10 microfarads.

The use of a conventional capacitance bridge for the measurement of condenser capacities prior to their connection into the analogue circuit has been found unsatisfactory in most cases. The conventional bridge measures the capacitance in an alternating-current circuit, whereas the condensers are used in a direct-current circuit. Most paper and oil-filled condensers exhibit a characteristic when charged termed "dielectric absorption." Instead of merely a surface charge forming on the condenser plates, the dielectric apparently becomes permeated with the charge also. There is some resistance to the permeation process which increases the time for charging and discharging of the condenser. The effective direct-current capacitance, therefore, must be determined from charging or discharging curves for each condenser when connected in an RC circuit. The curves should be checked against theory inasmuch as a large degree of dielectric absorption can render a condenser useless for analogue applications.

Requirements for mounting panels.- The primary electrical requirement for the material of the panels used for mounting the electrical components is that it must have very high leakage resistance under all anticipated conditions of humidity and temperature. Tests have shown that clear methyl methacrylate resin is a very satisfactory material from this standpoint.

Requirements for measuring equipment.- The representative temperature difference and heat flow at any point in an analogue circuit may be determined from either a voltage measurement across a known resistance or a measurement of current flow through the resistance. There are certain requirements for each measuring technique. When voltage is measured, the resistance of the meter must be large relative to that of the analogue circuit. Because the resistance of most meters is comparatively low, the use of a cathode-follower circuit into which the meter is connected should provide the necessary measuring resistance.

When current is measured, the resistance of the meter must be small relative to that of the analogue circuit. Generally, the circuit resistances will be sufficiently high that standard meters can be used without difficulty.

Comparison of Calculated Values With Results From the Electric Model

In order to obtain a check on the accuracy of the electric model for the simulation of the flow of heated air in a wing, a problem was placed on the model for which the solution had been previously computed. The problem considered was the flow of heated air through a circular tube 8 inches long which was cooled externally. Surface temperatures along the length of the tube, as obtained by the two methods, provided the basis for establishing the accuracy of the analogue.

The heated air was assumed to enter the tube at a temperature of 300° F, and the coefficient of internal heat transfer was taken as 15 Btu/hr, ft², °F. An air-flow rate of 10 pounds per hour was assumed. The tube was considered to be 0.35-inch diameter with an infinitesimally thin wall. Heat conduction lengthwise, therefore, was neglected. The external coolant was considered to be at a temperature of 0° F, and the external coefficient of heat transfer was taken as 40 Btu/hr, ft², °F.

In computing values of tube-surface temperature for comparison with the solution by the electric model, a step-by-step procedure was employed. The tube was divided into 1-inch-lengthwise increments, and a balance of the heat removed from the air to that delivered to the surface was obtained for each increment.

For the electrical analogy, the tube was divided into 1-inch increments also. Three separate tests were made with different values of resistance, capacitance, and commutator rotational speed. These were as follows:

Test	R_{int}, megohms	R_{ext}, megohms	C, mfd	ω, rpm
1	2.34	0.874	0.508	90
2	1.17	0.437	0.508	180
3	1.17	0.437	1.01	90

The three tests should give identical results, provided the above values are maintained rigidly, since they satisfy equation (17b) and, hence, represent identically analogous conditions. Results of the three tests are presented in figure 14, which compares the tube-surface-temperature distribution as measured using the electric model with the calculated variation. The values for the three test arrangements agree with each other and with the calculated curve within 1° F. From these data, it may be concluded that the electric model provides sufficiently accurate results for thermal-system-design applications.

APPENDIX C

APPLICATION OF AN ELECTRIC MODEL TO THE ANALYSIS

OF AN AIR-HEATED WING FOR ICE PREVENTION

Conditions and Assumptions

Wing-geometry and internal conditions.- In order to illustrate the
application of the electrical-analogue system to the analysis of an air-
heated wing, a typical double-skin arrangement consisting of corrugated-
type passages was chosen. The wing geometry was taken as follows:

          Root section . . . . NACA 64_1-312   13-ft chord
          Tip section . . . . NACA 64-408   6-ft chord
          Angle of attack . . . . 0°

The analysis was performed only for the upper surface of the wing at
the root and tip stations. Cross sections of the wing leading-edge region
at the two stations are presented in figure 15. Details of the double-
skin corrugated passages also are shown in this figure. The required
chordwise extent of double-skin area was taken as 16 inches for the root
section and 9 inches for the tip. These correspond to 8.75- and 11.7-
percent chord, respectively, for the two stations. Normally, the required
chordwise extent of double skin would be calculated from knowledge of the
largest size of water drops expected, but for this example the values
were chosen arbitrarily.

For purposes of analysis, the wing was divided chordwise into 8 seg-
ments at the root and 6 at the tip, as illustrated in figure 15. Condi-
tions were taken as being uniform throughout each segment. The analysis
was performed for a 1-inch-wide spanwise strip encompassing a single cor-
rugation at each wing station.

The heated air was assumed to enter the wing-root corrugation at a
temperature of 400° F and an absolute static pressure of 1073 lb/ft^2.
Assuming full dynamic pressure of the air stream is available at the air
inlet to the thermal system, this represents a pressure drop of 63 lb/ft^2,
or about 40 percent of the dynamic pressure, up to the entrance of the
corrugation, for the airspeed and altitude conditions given below. At the
entrance to the wing-tip corrugation, the air temperature was taken as
380° F and the absolute static pressure as 1060 lb/ft^2.

In order to simplify the example, the transfer of heat from the air
in the leading-edge duct to the back of the corrugated skin was considered
negligible. This might be the case when a duct liner of insulating mate-
rial is used.

Flight, meteorological, and water-drop-impingement conditions.- The assumed airplane flight conditions are

True airspeed   350 mph
Pressure altitude   20,000 ft

It was assumed that the airplane was to be operated over the plateau area of the United States (fig. 3). Since high values of liquid-water content are critical for a wing thermal system, and since high water contents usually are associated with high air temperature, a temperature of 20° F was selected for the design condition. An exceedance probability of 1 in 100 icing encounters was taken as the design criterion, and the values of water content presented in reference 10 for this condition were modified for a 50-mile horizontal extent. The resulting relationship of liquid-water content and drop size is shown in figure 4.

In order to determine the critical meteorological condition for the wing, curves of constant rate of water-drop impingement for the wing-root section were plotted in figure 4. These were estimated from data presented in reference 11. In the interest of expedience, estimated curves were used rather than values computed from reference 16 inasmuch as these curves are satisfactory for illustrative purposes. From figure 4, it is seen that the critical condition for this section of the wing occurs at 0.24 gram per cubic meter and 20 microns. For purposes of illustration, it was assumed that this was also the critical condition for the wing-tip section, although it is unlikely that the same meteorological condition actually would be critical for both sections. The calculated total rates of water interception are 4.3 and 3.3 pounds per hour per foot span for the root and tip sections, respectively. The rearmost point of impingement for these conditions was taken as 6 inches from the stagnation point[2] for the root section and 4-1/2 inches for the tip section. The assumed distributions of impingement for the upper surface at the two stations are shown in figure 16. In constructing these curves, all the water striking the wing was considered to be divided equally between the upper and lower surfaces. The information contained in reference 16 was used as a guide in establishing the shape of the distribution curves.

Electrical circuit representing the air-heated wing.- The electrical circuit representing the thermal circuit of the air-heated wing considered in the application of the electric model is shown in figure 17. It will be noted that there are two locations of possible current measurement for each wing segment: one in the external-air-resistance circuit to provide a measure of surface-temperature rise, and one in the internal-air-resistance circuit to provide a measure of heated-air-temperature rise.

_____

[2]The stagnation point and wing leading edge in this case are coincident.

Calculation of Analogue Values

In determining the required values of resistance for the analogue circuit, it was decided to multiply all calculated values by a factor of 80. The reason for this is that it was considered desirable to reduce the computed values of Cω by this factor to obtain reasonable values of capacitance and commutator rotational speed. Since the resulting resistances are quite large, it is desirable to convert them in terms of megohms. Thus, from equations (15a) and (15b)

$$R = \frac{0.288\ L}{kA} \quad \text{megohms} \tag{22a}$$

or

$$R = \frac{0.288}{HA} \quad \text{megohms} \tag{22b}$$

For evaluation of capacitance and rotational speed, the specific heat of the heated air was assumed constant at a value of 0.243 Btu/lb, °F, corresponding to a temperature of 300 F. The number of commutator segments on the electric model is 12. If these values are substituted in equation (20) and a factor of 1/80 is included to satisfy equation (17b), the product Cω becomes

$$C\omega = 4.22\ w$$

The value of C was chosen as 0.508 mfd, because of the availability of condensers of this capacity.[3] As a result, the commutator rotational speed is given by

$$\omega = 8.31\ w \tag{23}$$

In establishing the required external- and internal-air resistances, charts depicting these resistance values were found useful. These, together with other charts and calculation procedures, are discussed below. In order to clarify the derivation of these charts, specific examples will

---

[3]Since there are 12 commutator segments, 12 condensers were required.

be shown. In these examples, segment 8 of the wing-root station will be chosen for illustration.

External-air-resistance chart.- The resistance to external heat flow from the wing surface is a function primarily of the convective heat-transfer coefficient and the rate of evaporation of water. Because the rate of evaporation is a function of surface temperature, the effective coefficient of heat transfer varies with surface temperature, and the analogue resistance representing this effective coefficient must vary likewise. To determine this variation, curves of unit heat flow as a function of surface temperature were constructed for each chordwise wing segment using equation (1) and taking average values for conditions prevailing over the segment. Solutions to equation (1) were obtained with the aid of the chart included in reference 30. Values of the convective heat-transfer coefficient h_a in equation (1) were determined by use of equations (3), (4), and (5). The curve of h_a calculated for the wing-root station is presented in figure 18. Transition was assumed to start at the end of the area of impingement, with a gradual transitional region following. The value for the wetness fraction K in equation (1) was taken as 1 in the impingement area. Aft of this area, the values of K given in figure 5 were used.

A curve of the heat-flow variation for wing segment 8 is shown in figure 19 and was constructed as follows. For this segment, the following conditions apply:

$$M_w = 0 \text{ lb/hr, ft}^2$$
$$h_a = 36 \text{ Btu/hr, ft}^2, {}^\circ F$$
$$t_O = 20^\circ F$$
$$V_O = 514 \text{ ft/sec}$$
$$p_l = 12.75 \text{ in. Hg}$$
$$p_O = 13.75 \text{ in. Hg}$$
$$K = 0.15$$

From the above values and the chart of reference 30, the heat-transfer rate q was computed for the expected range of surface temperatures.

The effective heat-transfer coefficients at several temperatures were obtained from the heat-flow curves by use of the relation

$$H = \frac{q}{t_s - t_d}$$

in which t_d represents the surface temperature when q is zero. Then, by substitution of these values in equation (22b), curves of R_a vs. t_s

for each segment were obtained. The curve of resistance as a function of surface temperature for segment 8 is given in figure 20.

Internal-air-resistance chart.- The resistance to heat flow from the internal heated air to the walls of the air passages is a function of the weight flow of air and the distance from the passage entrance. Values of the coefficient h_{a_p} were computed for each segment for a range of air-flow rates from equations (6) and (7), and the electrical resistance as a function of flow rate was obtained for each segment by use of equation (22b) where $H = h_{a_p}$. These data were computed for both the outer-skin surface and the inner-skin surface.

For the case of segment 8, equation (7) was applied, inasmuch as this segment is beyond the entrance region of 25 hydraulic diameters. Figure 21 presents the internal-air-resistance curves for segment 8. In the calculation of these curves, the values of k and μ (conductivity and viscosity) for air were taken as constant and were evaluated at a temperature of 300° F.

Calculation of other resistance values.- The electrical resistances representing the thermal resistances in the aluminum skins, both inner and outer, were computed by use of equation (22a), where L represents the effective distance along the skin in the direction of heat flow. The value of k in equation (22a) was taken as 67.7 Btu/hr, ft^2, $^\circ$F/ft, representative of 24 ST aluminum alloy.

To establish the resistance between the inner and outer skins at the joints, equation (22b) was used, in which k_j, the conduction coefficient, was substituted for H. The value of k_j was taken as 55 Btu/hr, ft^2, $^\circ$F, as suggested in reference 36.

Rate-of-evaporation chart.- The determination of the rate of evaporation from the wing surface was facilitated by the use of curves of M_{ev} as a function of t_s, which were constructed for each segment with the aid of equation (2) and reference 30. The values of h_a and K were the same as used in the calculations for the external-air-resistance chart. A plot of the rate of evaporation as a function of surface temperature for segment 8 is illustrated in figure 22.

The total rate of evaporation from the entire heated area is given as the summation of the individual rates for each segment, or

$$M_{ev_T} = M_{ev_1}\Delta L + M_{ev_2}\Delta L + \ldots + M_{ev_n}\Delta L$$

Thus,

$$M_{ev_T} = \Delta L(M_{ev_1} + M_{ev_2} + \cdots + M_{ev_n}) \tag{24}$$

The term ΔL represents the length of surface distance for each segment, and the subscript numbers designate the appropriate segments.

Heated-air pressure-loss chart.- Curves of the parameter $\Delta P/v_{av}$ as a function of air-flow rate for the wing-root and -tip upper-surface corrugations were computed from equation (10), and are shown in figure 23. The term ΔP represents the total pressure drop in inches of water for each entire corrugation.

<div align="center">

Procedure for Determining Required
Heated-Air-Flow Rate
</div>

The procedure for determining the required heated-air-flow rate utilizing the electric model will now be considered. To satisfy the basic requirement for adequate ice protection, as previously set forth herein, it is necessary to evaporate all impinging water under the design condition. This is accomplished by a trial-and-error procedure involving two basic steps, as mentioned previously. These are (1) to obtain the surface-temperature distribution for an assumed air-flow rate, and (2) to compute the total rate of evaporation for this temperature distribution. This procedure will be demonstrated for the wing-root station.

Initial estimates.- In order to set the appropriate values of external-air resistance on the model, it is first necessary to estimate the values of surface temperature, in view of the fact that the value of resistance is dependent upon temperature. An initial estimate of the approximate magnitude of temperature in the leading-edge region can be obtained by calculating the surface temperature required to maintain a dry surface. In this case,

$$e_s = e_l + \frac{M_w p_l c_p}{0.622 h_a} \tag{25a}$$

where e_s represents the water-vapor pressure at temperature t_s. The contribution of e_l is small and, for estimation purposes, can be neglected. This leads to

$$e_s = \frac{M_w p_l c_p}{0.622 h_a} \tag{25b}$$

For segment 1 of the root section, the following average values apply:

$$M_w = 8.25 \text{ lb/hr, ft}^2$$
$$p_l = 14.8 \text{ in. Hg}$$
$$c_p = 0.245 \text{ Btu/lb, }^\circ\text{F}$$
$$h_a = 20 \text{ Btu/hr, ft}^2, ^\circ\text{F}$$

The resulting value of e_s is found to be 2.40 in. Hg, and the corresponding value of t_s is 107° F. It is not necessary, however, to maintain a dry surface (i.e., evaporate all intercepted water in the area of impingement) because some evaporation will be obtained in the heated region aft of the impingement area. Therefore, the surface temperature of segment 1 can be somewhat less than 107° F. As an initial estimate, a value of 85° F was chosen. The surface temperatures for the remainder of the segments were then estimated, bearing in mind the magnitude of the external-air resistances and the probable decrease in temperature of the heated air as it proceeds through the corrugation. A rough check of the appropriateness of these values of surface temperature was obtained by computation of the total rate of evaporation with the help of the evaporation charts and equation (24). The initial estimate of the surface temperatures, together with the corresponding resistances and evaporation rates are tabulated below.

Segment number	$t_s,$ $^\circ$F	$R_a,$ megs	M_{ev} lb/hr, ft^2
1	85	0.12	3.9
2	90	.18	2.9
3	95	.22	2.7
4	90	.37	1.3
5	70	.28	1.0
6	60	.29	.6
7	55	.35	.4
8	50	.43	.3

The sum of the M_{ev} values is 13.1 and, since $\triangle L$ equals 2 inches, or 0.167 foot, the total rate of evaporation, from equation (24), equals 2.18 lb/hr, ft. Since the required rate of evaporation must equal the rate of impingement, or $1/2 \times 4.3 = 2.15$ lb/hr, ft, the above estimated surface temperatures appear to be of the right order of magnitude, and the corresponding external-air resistances were used in the initial test.

The required heated-air-flow rate must be determined by a trial-and-error procedure in which a value of w is assumed, the resulting surface-temperature distribution is obtained by use of the electric model, and the corresponding evaporation rate is computed. The procedure is repeated, if necessary, until the rate of evaporation is made to equal the rate of impingement.

Calculated values.- The value of heated-air-flow rate taken for the initial test was 10 lb/hr per corrugation. The electric model was adjusted for the corresponding internal-air-resistance values. From equation (23), the commutator rotational speed representative of the flow rate is found to be 83 rpm. The initial test performed using these values produced the surface temperatures listed in the following table:

Segment number	First estimate				Measured, first test		Second estimate		Measured, second test		
	t_s, °F	R_a, megs	R_{a_p}, outer, megs	R_{a_p}, inner, megs	Δt_s, °F	t_s, °F	t_s, °F	R_a, megs	Δt_s, °F	t_s, °F	M_{ev}, lb/hr, ft²
1	85	0.12	0.69	0.58	60	80	82	0.125	61.5	81.5	3.5
2	90	.18	.97	.82	61.5	81.5	85	.20	64.5	84.5	2.45
3	95	.22	1.14	.95	61	81	87	.25	66	86	2.05
4	90	.37	1.17	1.00	78	98	95	.35	74	94	1.45
5	70	.28	1.17	1.00	58	78	75	.27	55	75	1.15
6	60	.29	1.17	1.00	54.5	74.5	69	.26	49.5	69.5	.95
7	55	.35	1.17	1.00	54	74	68	.29	48	68	.75
8	50	.43	1.17	1.00	52.5	72.5	66	.39	46	66	.6

It is seen that the measured temperatures differ from the initially estimated temperatures. Because of this, the values of resistance used in the test are not appropriate for the measured temperatures. The correct temperatures, therefore, lie between the estimated and measured values, and it was necessary to make a second estimate of surface temperature and, by use of the corresponding resistance values, to perform a second series of measurements. These latter estimates and measurements are given in the above table. Good agreement now exists between the measured and estimated temperatures, signifying that the correct values of resistance were employed and, hence, the measured temperatures are correct.

For these measurements, the value of R_{a_d} in equation (21) was chosen as 0.7 megohm, and the measured value of I_{a_d} was 28.7 microamperes when the battery voltage was impressed across R_{a_d}. During the first test, the measured value of I for segment 1 was 26.5 microamperes and, as noted in the table, R_a was 0.12 megohm. Then, since t_{a_d} was

assumed to be 400° F, Δt_{a_d} equals 380° F, and Δt_s from equation (21) is 60° F; thus, t_s equals 80° F. The remainder of the surface-temperature values were computed from the measurements in the same manner.

The rates of evaporation for each segment were obtained from the rate-of-evaporation charts for the corresponding surface temperatures and are presented in the above table. Substitution of these values in equation (24) yields $M_{ev_T} = 2.15$ lb/hr, ft, which also is the value of the rate of water impingement. Thus, the required heated-air-flow rate for the upper corrugation at the wing-root station is 10.0 lb/hr at an inlet temperature of 400° F.

The measured air temperature at the corrugation outlet was 185° F. By use of this value, together with the assumed inlet air temperature and average pressure, the average specific volume of the air in the corrugation was computed as 39.1 ft^3/lb. The air-pressure loss through the corrugation was determined from the pressure-loss chart for this value of v_{av} and was found to be 19.0 inches of water.

By the same procedure, the required air-flow rate for the tip section was established as 10.8 lb/hr per corrugation at an inlet temperature of 380° F. The resulting pressure drop was calculated to be 13.2 inches of water, which means that the pressure loss in the leading-edge duct from the wing root to the tip could be about 6 inches of water.

REFERENCES

1. Jones, Alun R., and Rodert, Lewis A.: Development of Thermal Ice-Prevention Equipment for the B-24D Airplane. NACA WR A-35, 1943. (Formerly NACA ACR, Feb. 1943)

2. Jones, Alun R., and Rodert, Lewis A.: Development of Thermal Ice-Prevention Equipment for the B-17F Airplane. NACA WR A-51, 1943. (Formerly NACA ARR No. 3H24)

3. Neel, Carr B., Jr.: An Investigation of a Thermal Ice-Prevention System for a C-46 Cargo Airplane. I - Analysis of the Thermal Design for Wings, Empennage, and Windshield. NACA WR A-52, 1945. (Formerly NACA ARR No. 5A03)

4. Hardy, J. K. (R.A.E.): An Analysis of the Dissipation of Heat in Conditions of Icing from a Section of the Wing of the C-46 Airplane. NACA Rep. 831, 1945. (Formerly NACA ARR 4I11a)

5. Hardy, J. K.: Protection of Aircraft Against Ice. Rep. No. S.M.E. 3380, British R.A.E., July 1946.

6. Tribus, Myron, and Tessman, J. R., editors: Report on the Development and Application of Heated Wings, Addendum I. Tech. Rep. 4972 (add. 1), AAF Air Materiel Command, Wright Field, Dayton, Ohio, Jan. 1946. (Available from Office of Technical Services, U. S. Department of Commerce as PB No. 18122.)

7. Neel, Carr B., Jr., Bergrun, Norman R., Jukoff, David, and Schlaff, Bernard A.: The Calculation of the Heat Required for Wing Thermal Ice Prevention in Specified Icing Conditions. NACA TN 1472, 1947.

8. Jones, Alun R., Holdaway, George H., and Steinmetz, Charles P.: A Method for Calculating the Heat Required for Windshield Thermal Ice Prevention Based on Extensive Flight Tests in Natural Icing Conditions. NACA TN 1434, 1947.

9. Gray, Vernon H. and von Glahn, Uwe H.: Effect of Ice and Frost Formations on Drag of NACA 65_1-212 Airfoil for Various Modes of Thermal Ice Protection. NACA TN 2962, 1953.

10. Lewis, William, and Bergrun, Norman R.: A Probability Analysis of the Meteorological Factors Conducive to Aircraft Icing in the United States. NACA TN 2738, 1952.

11. Hacker, P. T., and Dorsch, Robert G.: A Summary of Meteorological
    Conditions Associated with Aircraft Icing and a Proposed Method
    of Selecting Design Criterions for Ice-Protection Equipment.
    NACA TN 2569, 1951.

12. Langmuir, Irving, and Blodgett, Katharine B.: A Mathematical Investi-
    gation of Water Droplet Trajectories. Tech. Rep. 5418, AAF Air
    Materiel Command, Wright Field, Dayton, Ohio, Feb. 19, 1946.
    (Contract No. W-33-038-ac-9151 with Gen. Elec. Co.)

13. Bergrun, Norman R.: A Method for Numerically Calculating the Area
    and Distribution of Water Impingement on the Leading Edge of an
    Airfoil in a Cloud. NACA TN 1397, 1947.

14. Guibert, A. G., Janssen, E., and Robbins, W. M.: Determination of
    Rate, Area, and Distribution of Impingement of Waterdrops on
    Various Airfoils from Trajectories Obtained on the Differential
    Analyzer. NACA RM 9A05, 1949.

15. Tribus, M., and Rauch, L. L.: A New Method for Calculating Water-
    Droplet Trajectories about Streamlined Bodies. Univ. of Mich.,
    Engr. Res. Inst., Dec. 1951. (Proj. M992-E)

16. Bergrun, Norman R.: An Empirically Derived Basis for Calculating
    Area, Rate, and Distribution of Water-Drop Impingement on Airfoils.
    NACA Rep. 1107, 1952.

17. Tribus, Myron: Modern Icing Technology. Chapter II. Univ. of
    Mich., Engr. Res. Inst., Jan. 1952. (Proj. M992-E)

18. Sherman, P., Klein, J. S., and Tribus, M.: Determination of Drop-
    Trajectories by Means of an Extension of Stokes' Law. Univ. of
    Mich., Engr. Res. Inst., Apr. 1952. (Proj. 992-D)

19. Tribus, Myron, and Guibert, Armand: Impingement of Spherical Water
    Droplets on a Wedge at Supersonic Speeds in Air. Jour. Aero. Sci.,
    vol. 19, no. 6, June 1952, pp. 391-394.

20. Brun, E., and Vasseur, M.: The Mechanics of Suspensions. Univ. of
    Mich., Engr. Res. Inst., Nov. 1952. (Proj. M992-4) Trans. from:
    Jour. des Recherches du Centre National de la Recherche Scientifique
    no. 3, 1947, pp. 107-122.

21. Lenherr, F. E., and Thomson, J. E.: Report on the Computation of
    Water Drop Trajectories About a Six Percent Airfoil at Zero and
    Four Degrees Angles of Attack. TDM-67A, Northrop Aircraft, Inc.,
    Hawthorne, Calif., Oct. 6, 1952.

22. Brun, Rinaldo J., Serafini, John S., and Moshos, George J.: Impingement of Water Droplets on an NACA 65_1-212 Airfoil at an Angle of Attack of 4°. NACA RM E52B12, 1952.

23. Tribus, Myron: The Trajectories of Water Drops. Univ. of Mich. Airplane Icing Information Course, Lecture No. 3, 1953.

24. Brun, Rinaldo J., Serafini, John S., and Gallagher, Helen M.: Impingement of Cloud Droplets on Aerodynamic Bodies as Affected by Compressibility of Air Flow Around the Body. NACA TN 2903, 1953.

25. Dorsch, Robert G., and Brun, Rinaldo J.: A Method for Determining Cloud-Droplet Impingement on Swept Wings. NACA TN 2931, 1953.

26. Brun, Rinaldo J., Gallagher, Helen M., and Vogt, Dorothea: Impingement of Water Droplets on NACA 65_1-208 and 65_1-212 Airfoils at 4° Angle of Attack. NACA TN 2952, 1953.

27. Serafini, John S.: Impingement of Water Droplets on Wedges and Diamond Airfoils at Supersonic Speeds. NACA TN 2971, 1953.

28. Brun, Rinaldo J., Gallagher, Helen M., and Vogt, Dorothea E.: Impingement of Water Droplets on NACA 65A004 Airfoil and Effect of Change in Airfoil Thickness from 12 to 4 Percent at 4° Angle of Attack. NACA TN 3047, 1953.

29. Neel, Carr B., Jr.: Calculation of Heat Required for Wing Thermal Ice Prevention in Specified Icing Conditions. S.A.E. Quart. Trans., vol. 2, no. 3, July 1948, pp. 369-378.

30. Gray, Vernon H.: Simple Graphical Solution of Heat Transfer and Evaporation from Surface Heated to Prevent Icing. NACA TN 2799, 1952.

31. Messinger, Bernard L.: Equilibrium Temperature of an Unheated Icing Surface as a Function of Air Speed. Jour. Aero. Sci., vol. 20, no. 1, Jan. 1953, pp. 29-42.

32. Boelter, L. M. K., Grossman, L. M., Martinelli, R. C., and Morrin, E. H.: An Investigation of Aircraft Heaters. XXIX - Comparison of Several Methods of Calculating Heat Losses from Airfoils. NACA TN 1453, 1948.

33. Martinelli, R. C., Guibert, A. G., Morrin, E. H., and Boelter, L. M. K.: An Investigation of Aircraft Heaters. VIII - A Simplified Method for the Calculation of the Unit Thermal Conductance Over Wings. NACA WR W-14, 1943. (Formerly NACA ARR, Mar. 1943)

34. Boelter, L. M. K., Martinelli, R. C., Romie, F. E., and Morrin, E. H.: An Investigation of Aircraft Heaters. XVIII - A Design Manual for Exhaust Gas and Air Heat Exchangers. NACA WR W-95, 1945. (Formerly NACA ARR 5A06)

35. Gelder, Thomas F., and Lewis, James P.: Comparison of Heat Transfer from Airfoil in Natural and Simulated Icing Conditions. NACA TN 2480, 1951.

36. Hardy, J. K., and Morris, R.: Transfer of Heat Internally in a Heated Wing. Rep. No. Mech. Eng. 4, British R.A.E., Jan. 1948.

37. Bowers, R. D., ed.: Icing Report by the University of California, Fiscal Year 1946. AAF Tech. Rep. 5529, Section II, AAF Air Materiel Command, Wright Field, Dayton, Ohio, Nov. 1946.

38. Hauger, Harry H., Jr.: Intermittent Heating of Airfoils for Ice Protection Utilizing Hot Air. Appendix F. M.S. Thesis, Univ. of Calif., Los Angeles, Dept. of Engr., 1953.

39. Brunot, A. W., and Buckland, Florence F.: Thermal Contact Resistance of Laminated and Machined Joints. A.S.M.E. Trans., vol. 71, no. 3, Apr. 1949.

40. Weills, N. D., and Ryder, E. A.: Thermal Resistance Measurements of Joints Formed Between Stationary Metal Surfaces. A.S.M.E. Trans., vol. 71, no. 3, Apr. 1949.

41. McAdams, William Henry: Heat Transmission. 2nd Ed., McGraw-Hill Book Co., Inc., 1942.

42. Naiman, J. M.: Basic Principles Used in the Design of the Thermal Anti-Icing System of the DC-6 Airfoils. Douglas Aircraft Co., Rep. No. SM-11911, 1946.

43. Patterson, D. M.: A Simplified Procedure for the Determination of Heat Requirements for Ice Protection of Fixed Areas of Aircraft. Technical Data Digest (Central Air Documents Office), 15 Feb. 1949. pp. 15-23.

44. Lewis, James P., and Blade, Robert J.: Experimental Investigation of Radome Icing and Icing Protection. NACA RM E52J31, 1953.

45. Lenherr, F. E., and Young, R. W.: Computation of Water Catch on Axial Symmetric Aircraft Radomes. TDM-77, Northrop Aircraft, Inc., Dec. 17, 1952. (Prog. Rep. III, AF33(038)-1817)

46. Torgeson, W. L., and Abramson, A. E.: A Study of Heat Requirements
     for Anti-Icing Radome Shapes with Dry and Wet Surfaces. W.A.D.C.
     Tech. Rep. 53-284, Research, Incorporated, 1953.

47. Dorsch, Robert G., Brun, Rinaldo J., and Gregg, John L.: Impinge-
     ment of Water Droplets on an Ellipsoid with Fineness Ratio 5 in
     Axisymmetric Flow. NACA TN 3099, 1954.

48. Brun, Rinaldo J., and Dorsch, Robert G.: Impingement of Water
     Droplets on an Ellipsoid with Fineness Ratio 10 in Axisymmetric
     Flow. NACA TN 3147, 1954.

49. Frick, Charles W., Jr., and McCullough, George B.: A Method for
     Determining the Rate of Heat Transfer from a Wing or Streamline
     Body. NACA Rep. 830, 1945.

50. von Glahn, U.: Preliminary Results of Heat Transfer from a Stationary
     and Rotating Ellipsoidal Spinner. NACA RM E53F02, 1953.

51. Xenakis, G., Amerman, A. E., and Michelson, R. W.: An Investigation
     of the Heat-Transfer Characteristics of Spheres in Forced Convec-
     tion. W.A.D.C. Tech. Rep. 53-117, Smith, Hinchman & Grylls, Inc.
     (Ypsilanti, Mich.) Aeronautical Icing Research Lab., 1953.

52. Lewis, James P.: An Analytical Study of Heat Requirements for Icing
     Protection of Radomes. NACA RM E53A22, 1953.

53. Gray, Vernon H.: Improvements in Heat Transfer for Anti-Icing of
     Gas-Heated Airfoils with Internal Fins and Partitions. NACA
     TN 2126, 1950.

54. Gray, V. H., and Campbell, R. G.: A Method for Estimating Heat
     Requirements for Ice Prevention on Gas-Heated Hollow Propeller
     Blades. NACA TN 1494, 1947.

55. Mulholland, Donald R., and Perkins, Porter J.: Investigation of
     Effectiveness of Air-Heating a Hollow Steel Propeller for Protec-
     tion Against Icing. I - Unpartitioned Blades. NACA TN 1586, 1948.

56. Perkins, Porter J., and Mulholland, Donald R.: Investigation of
     Effectiveness of Air-Heating a Hollow Steel Propeller for Protec-
     tion Against Icing. II - 50-Percent Partitioned Blades. NACA
     TN 1587, 1948.

57. Mulholland, Donald R., and Perkins, Porter J.: Investigation of
     Effectiveness of Air-Heating a Hollow Steel Propeller for Protec-
     tion Against Icing. III - 25-Percent Partitioned Blades. NACA
     TN 1588, 1948.

58. Darsow, John F., and Selna, James: A Flight Investigation of the Thermal Performance of an Air-Heated Propeller. NACA TN 1178, 1947.

59. Neel, Carr B., Jr., and Bright, Loren G.: The Effect of Ice Formations on Propeller Performance. NACA TN 2212, 1950.

60. Patterson, G. N.: The Design of Aeroplane Ducts. Aircraft Engineering, vol. XI, no. 125, July 1939, pp. 263-268.

61. Patterson, G. N.: Modern Diffuser Design. Aircraft Engineering, vol. X, no. 115, Sept. 1938, pp. 267-273.

62. Patterson, G. N.: Corner Losses in Ducts. Aircraft Engineering, vol. IX, no. 102, Aug. 1937, pp. 205-208.

63. Patterson, G. N.: Note on the Design of Corners in Duct Systems. R. & M. No. 1773, British A.R.C., 1937.

64. Rogallo, F. M.: Internal-Flow Systems for Aircraft. NACA Rep. 713, 1941.

65. Hacker, Paul T., Brun, Rinaldo J., and Boyd, Bemrose: Impingement of Droplets in 90° Elbows with Potential Flow. NACA TN 2999, 1953.

66. Jackson, Richard: An Investigation of a Thermal Ice-Prevention System for a C-46 Cargo Airplane. II - The Design, Construction, and Preliminary Tests of the Exhaust-Air Heat Exchanger. NACA WR A-25, 1945. (Formerly NACA ARR No. 5A03a)

67. Pinkel, Benjamin, Noyes, Robert N., and Valerino, Michael F.: Method for Determining Pressure Drop of Air Flowing Through Constant-Area Passages for Arbitrary Heat-Input Distributions. NACA TN 2186, 1950.

68. Hillendahl, Wesley H.: A Comparison of Analytically and Experimentally Determined Isothermal Pressure Losses in a Heat-Exchanger Installation. NACA WR A-26, 1945. (Formerly NACA ARR No. 5C19)

69. Paschkis, Victor, and Baker, H. D.: A Method for Determining Unsteady-State Heat Transfer by Means of an Electrical Analogy. A.S.M.E. Trans., vol. 64, no. 2, Feb. 1942, pp. 105-112.

70. Ellerbrock, Herman H., Jr., Schum, Eugene F., and Nachtigall, Alfred J.: Use of Electric Analogs for Calculation of Temperature Distribution of Cooled Turbine Blades. NACA TN 3060, 1953.

(I) CORRUGATED   (2) MODIFIED   (3) DOUBLE SKIN   (4) DIMPLED SKIN
    SKIN   CORRUGATED SKIN   WITH SPACERS

(a) TYPICAL DOUBLE-SKIN ARRANGEMENTS

(I) GAP AT LEADING EDGE   (2) GAPS AT REAR

(b) TYPICAL CORRUGATED-SKIN DESIGNS WITH TWO ARRANGEMENTS OF DUCT LINER
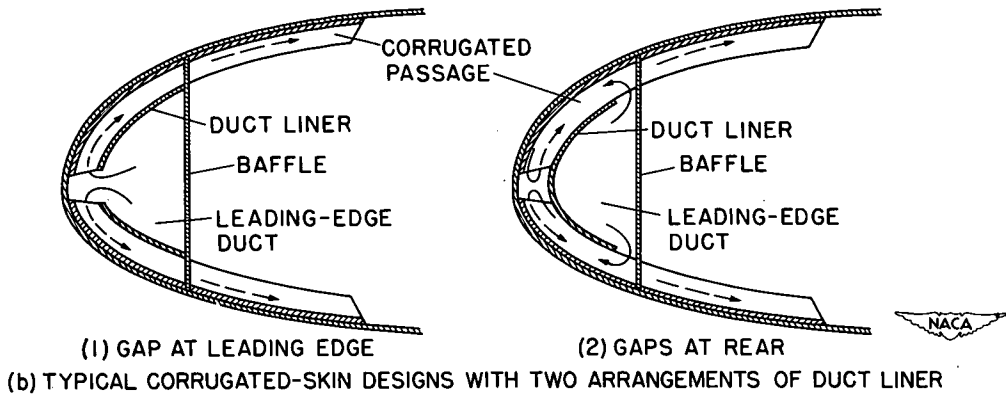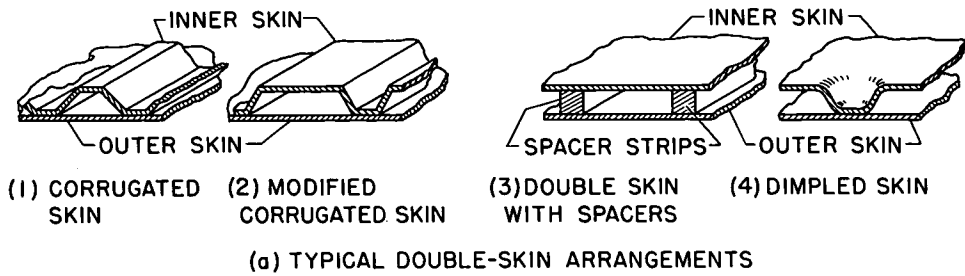
Figure 1.- Typical arrangements of double skin and leading-edge duct used
in air-heated wing systems for ice prevention.
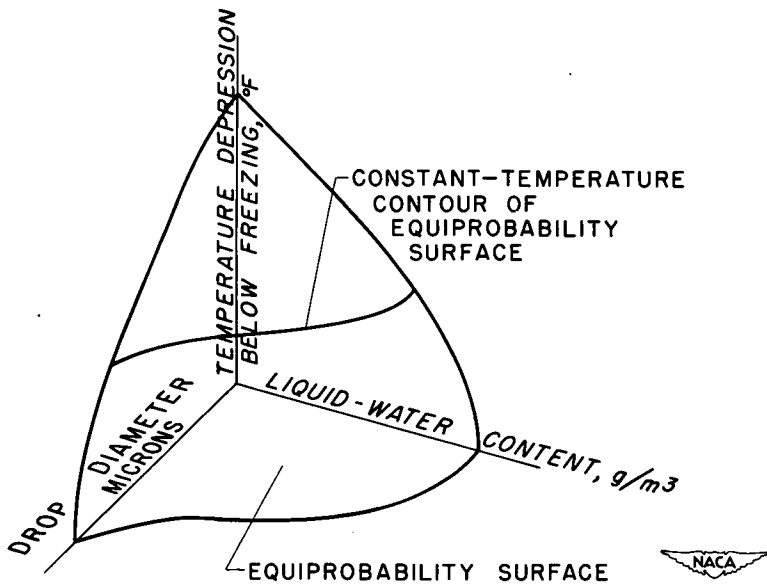
Figure 2.- Equiprobability surface defining meteorological conditions
having the same probability of being exceeded in any single icing
encounter.
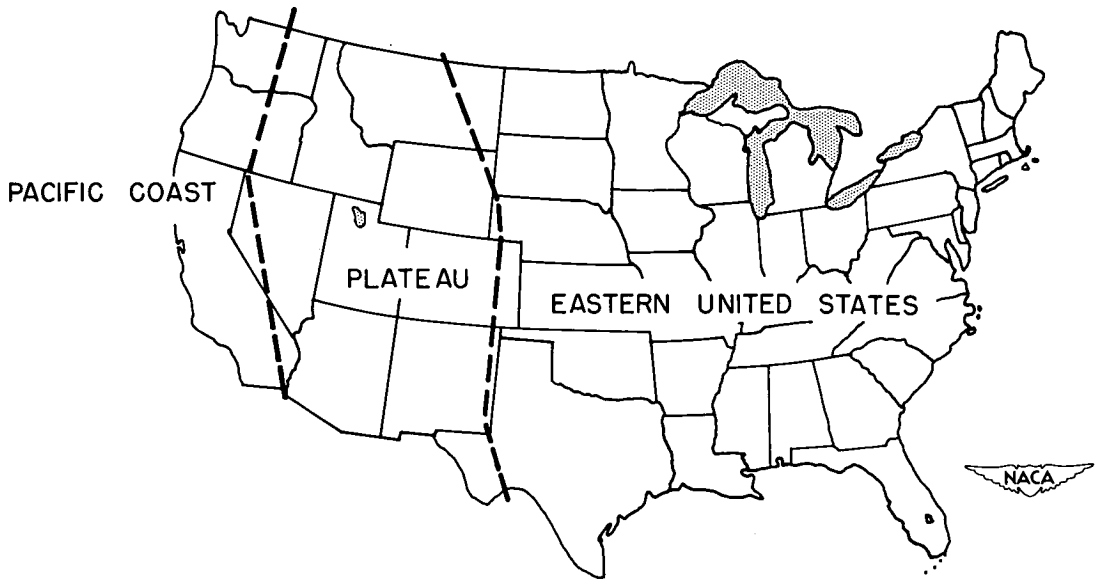
Figure 3.- Map of the United States showing boundaries of areas used
   in the geographical classification of icing data presented in
   reference 10.
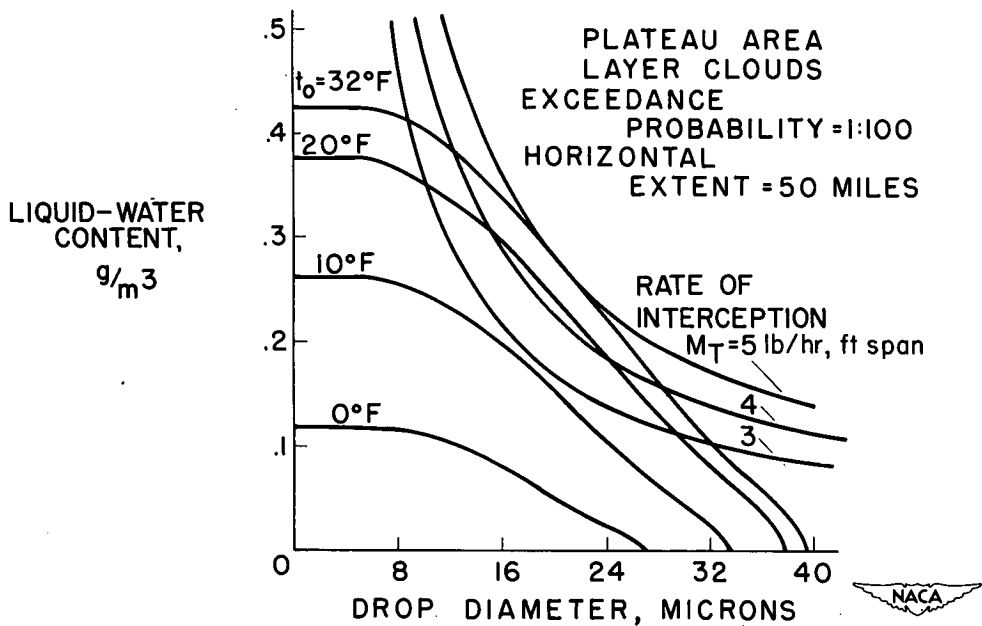
Figure 4.- Equiprobability surface and curves of constant rate of
   water interception for rapid evaluation of critical meteoro-
   logical conditions.
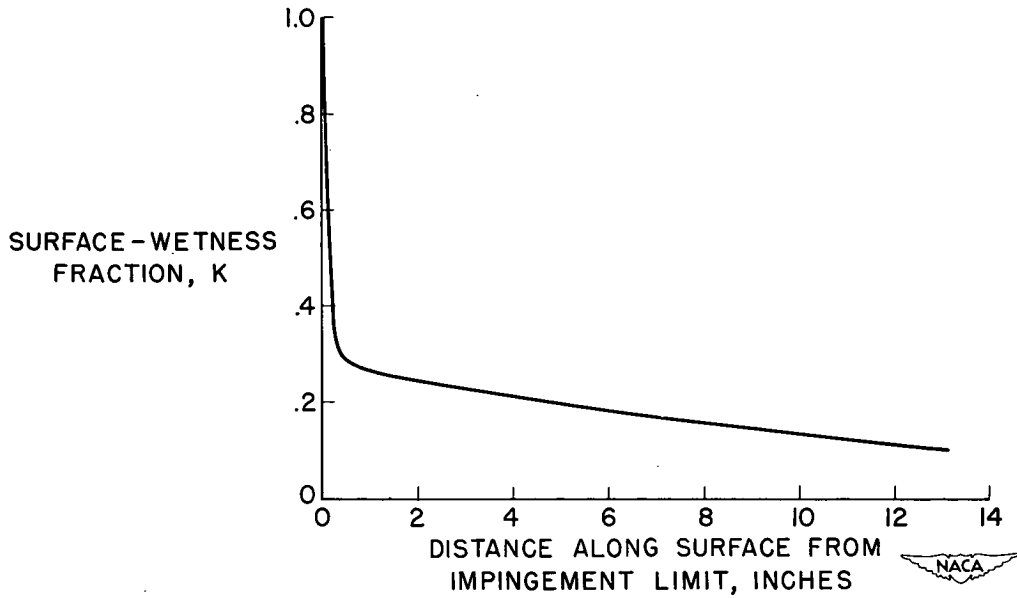
Figure 5.- Variation of wing-surface-wetness fraction aft of area of
water impingement with distance from limit of impingement.
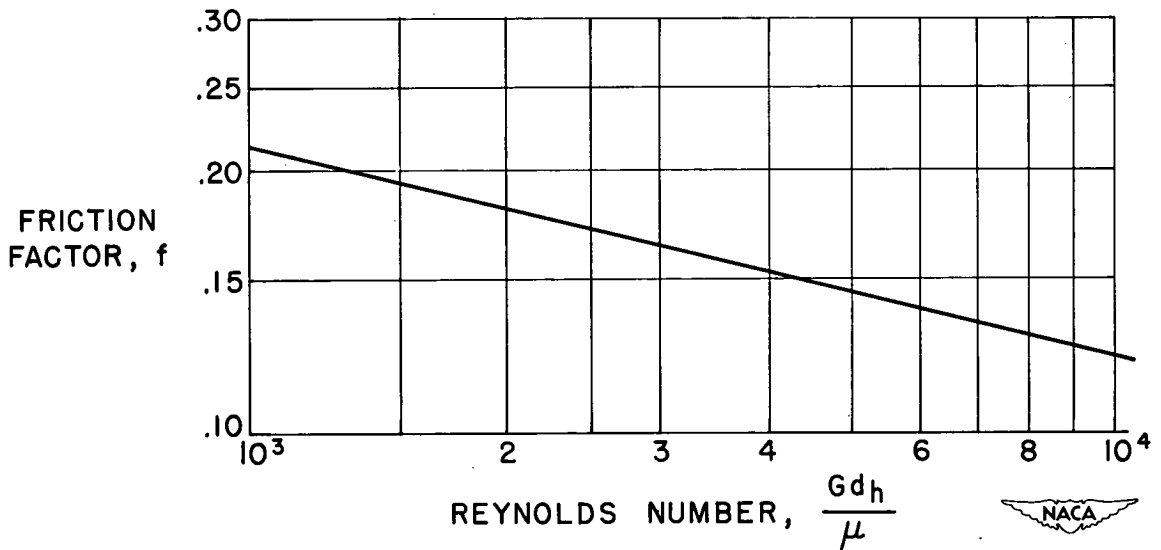
Figure 6.- Friction factor as a function of Reynolds number for
determining air-pressure losses in double-skin passages using
equation (10).
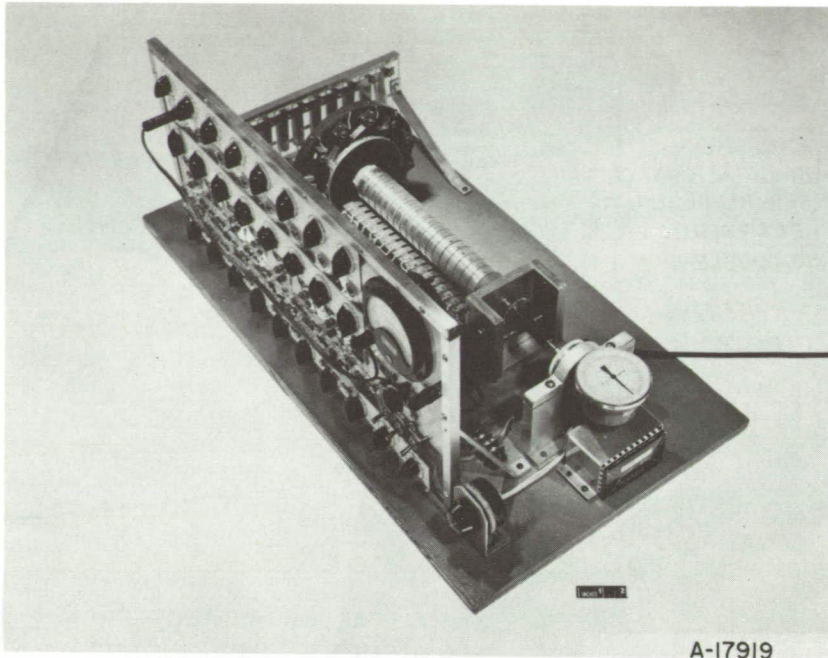
(a) PHOTOGRAPH OF COMPLETE MODEL
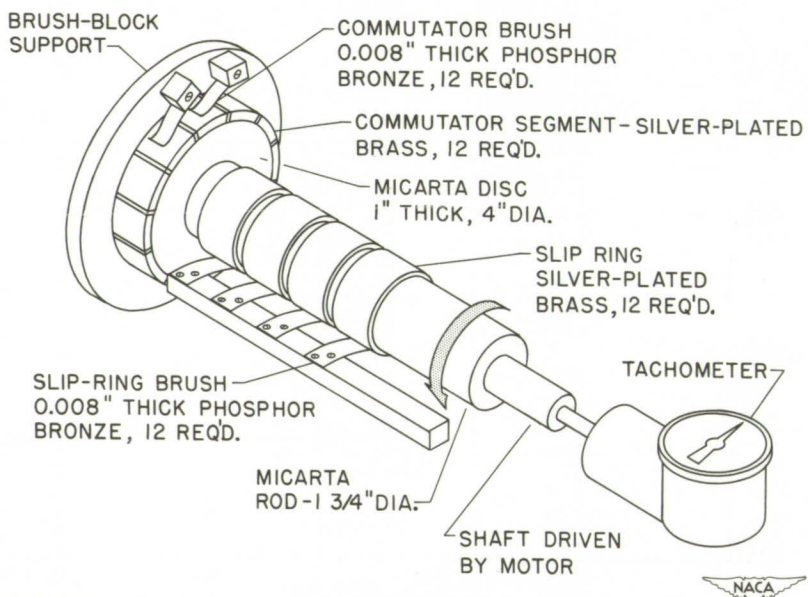
(b) SKETCH SHOWING DETAILS OF COMMUTATOR AND SLIP-RING ASSEMBLY

Figure 7.- Electric model used for simulating air-heated ice-prevention systems.

22-VOLT BATTERY—
PROVIDING INITIAL CHARGE TO
CONDENSER, REPRESENTING
INITIAL HEAT ENERGY OF AIR
ENTERING DOUBLE-SKIN
PASSAGE

BRUSH

COMMUTATOR SEGMENT

DIRECTION OF ROTATION

SLIP RING

E

BRUSH

VOLTAGE ACROSS RESISTANCE
REPRESENTS TEMPERATURE
RISE

RESISTORS, REPRESENTING
THERMAL RESISTANCE
FROM HEATED AIR—

CONDENSER, REPRESENTING
THERMAL CAPACITY OF
HEATED AIR

GROUND, REPRESENTING
FREE-AIR CONDITIONS—

Figure 8.- Simplified circuit diagram illustrating a portion of analogue
system for simulating the flow of heated air through a wing.
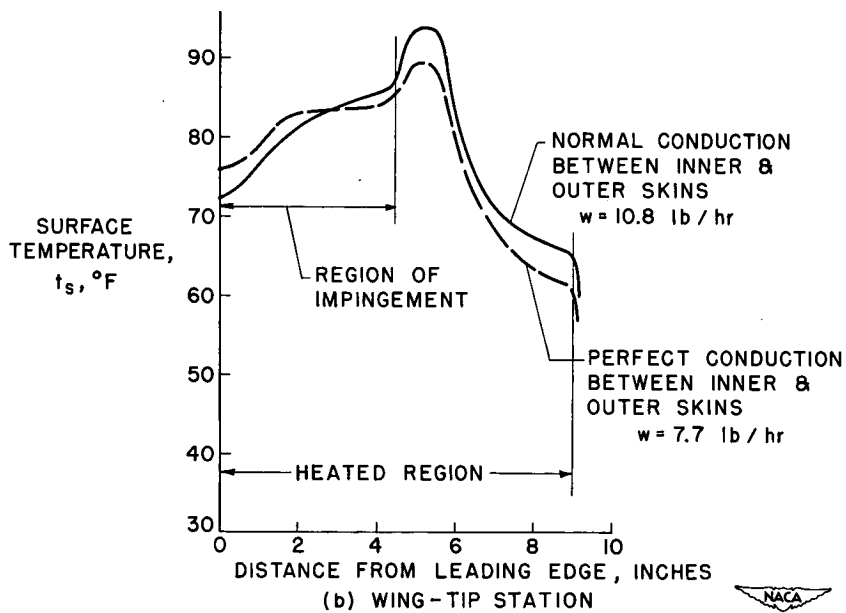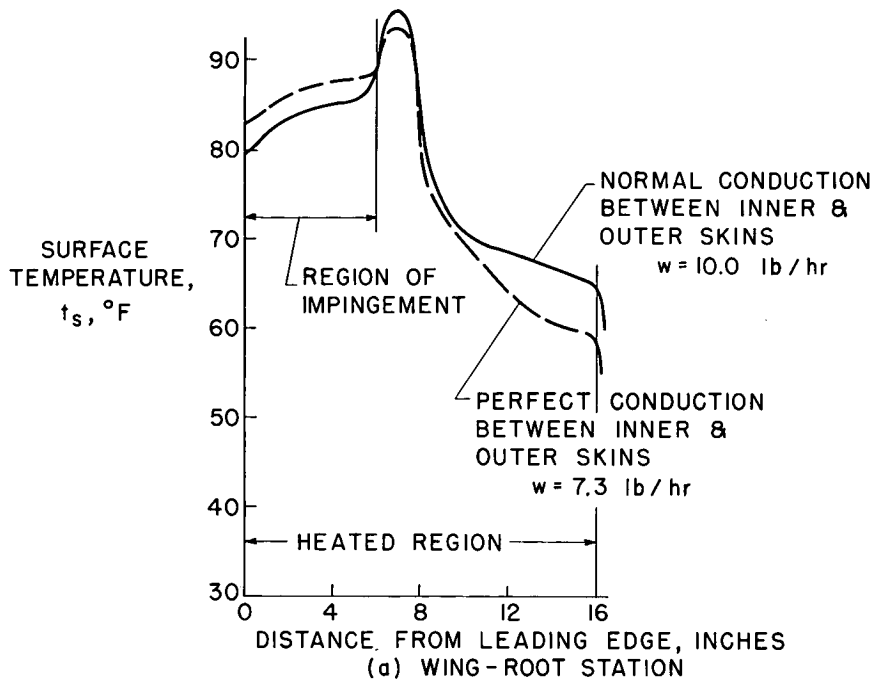
Figure 9.- Comparison of wing-surface-temperature distribution for two
conditions of conduction between inner and outer skins.
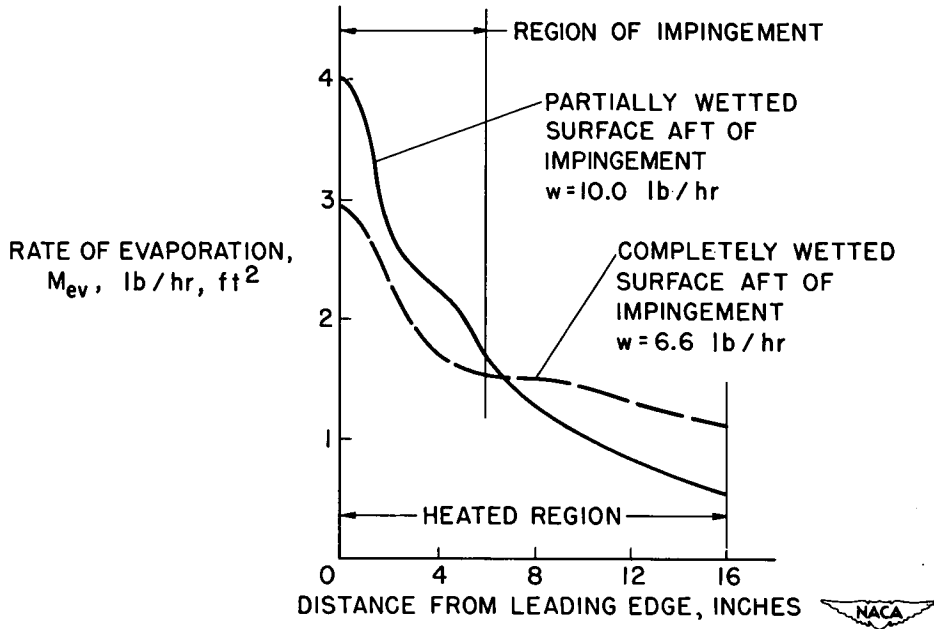
Figure 10.- Comparison of distribution of evaporation rate over wing surface for two conditions of surface wetness aft of impingement region.
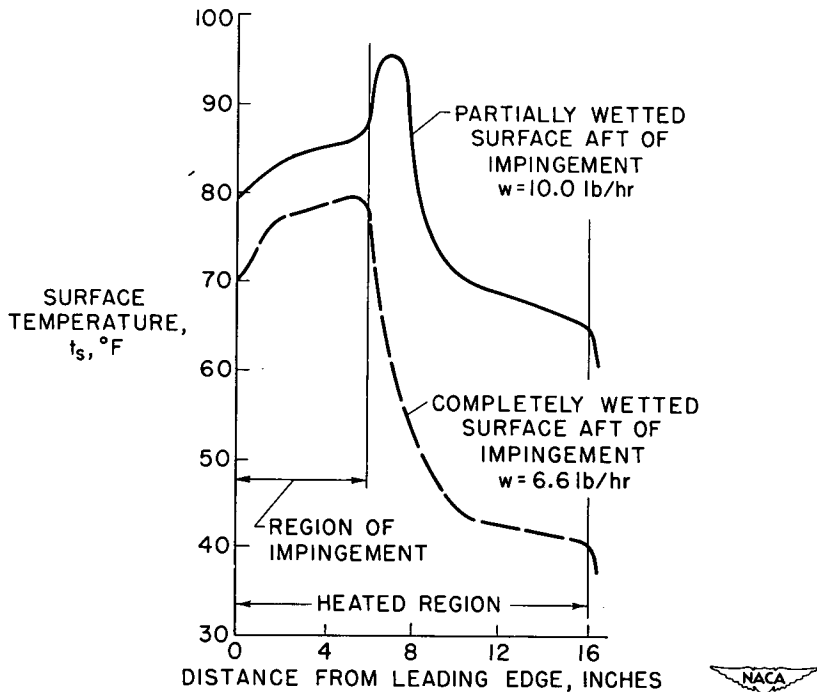
Figure 11.- Comparison of wing-surface-temperature distribution for two conditions of surface wetness aft of impingement region.

WINDSHIELD PANEL

1/2 RIBBON   STAGNATION STREAMLINE

(a) FLAT PLATE AND V-TYPE WINDSHIELDS

θ_M

FLUSH WINDSHIELD

MAX. DIA. OF FUSELAGE

STAGNATION STREAMLINE

SPHERE

(b) FLUSH WINDSHIELD
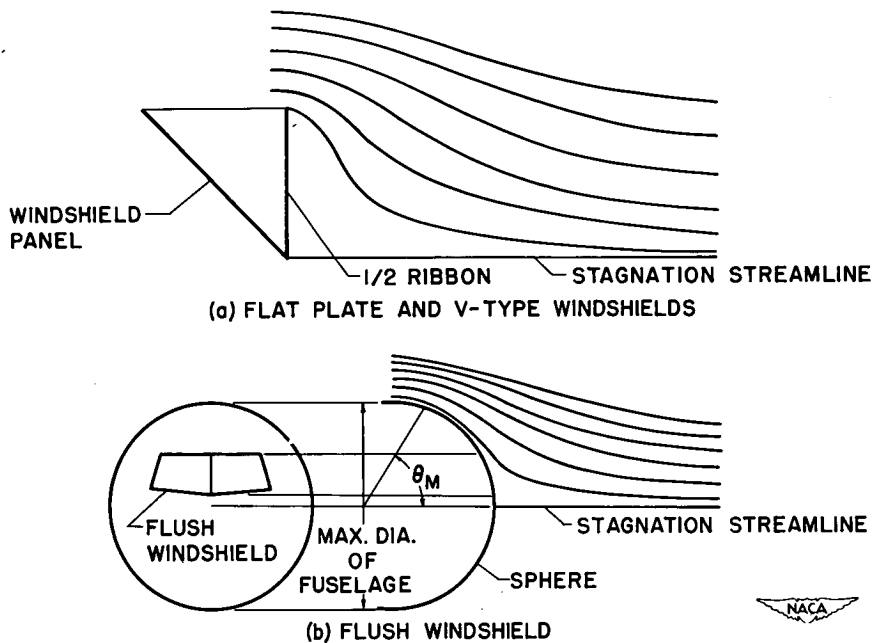
Figure 12.- Illustration of substitution procedure for calculating rate of water impingement on different types of windshields, using data for ribbons and spheres.

HEATED-AIR STREAMLINES

DIVISIONS FOR ANALYSIS

SEGMENTS MUST CONTAIN EQUAL VOLUMES OF HEATED AIR

INNER SHELL

OUTER HOUSING
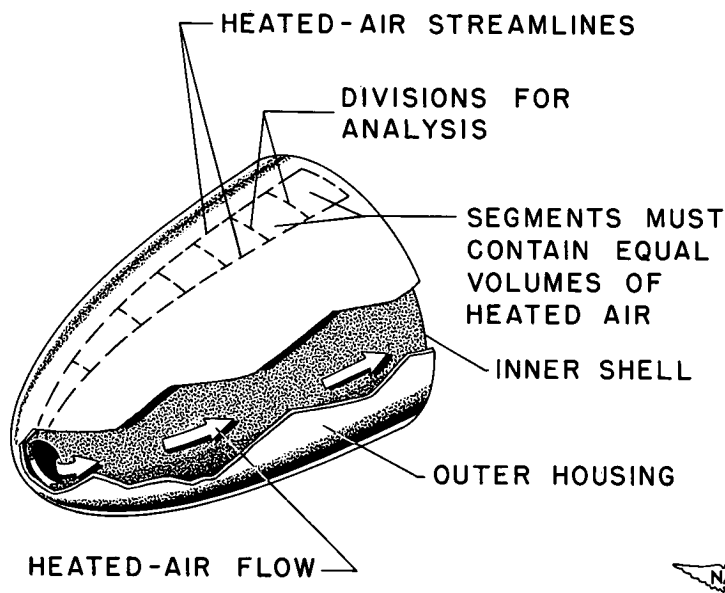
HEATED-AIR FLOW

Figure 13.- Proposed heating system for radome ice prevention and division of radome for analysis.
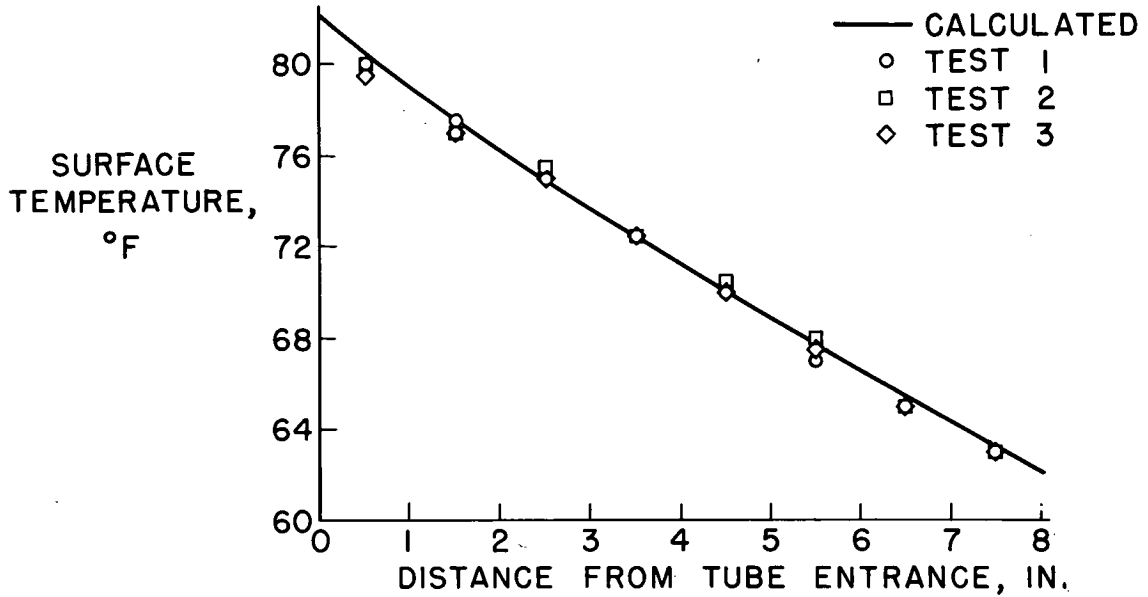
Figure 14.- Comparison of tube-surface-temperature distribution as calculated, and as measured using an electric model to simulate heated-air flow.

SEGMENT DESIGNATION

REGION OF
IMPINGEMENT
ON UPPER
SURFACE

-2"(TYP.)

DIVISIONS FOR ANALYSIS

CHORD LINE

.75"   .25   .025" 24 ST

.25   .2"

SEC. A-A
TYPICAL CORRUGATION
DETAIL
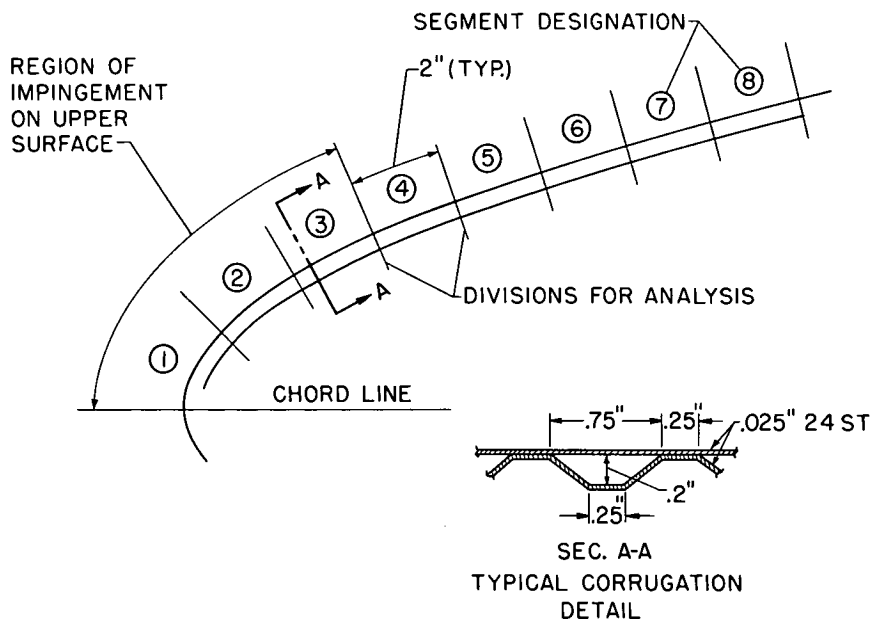
(a) WING-ROOT STATION
(NACA 64,-312 SECTION, 13-FT CHORD)

REGION OF
IMPINGEMENT
ON UPPER
SURFACE

1 1/2"(TYP.)

SEGMENT DESIGNATION

DIVISIONS FOR ANALYSIS

CHORD LINE
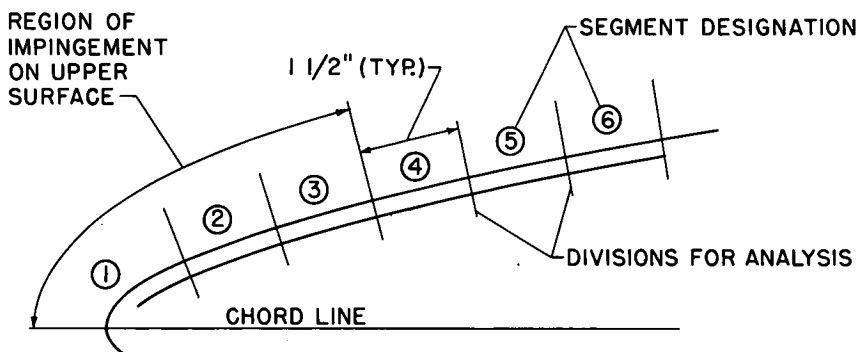
(b) WING-TIP STATION
(NACA 64-408 SECTION, 6-FT CHORD)

Figure 15.- Cross sections of forward region of wing upper surface chosen
    for analysis, showing chordwise divisions for use with electric model,
    and other details.
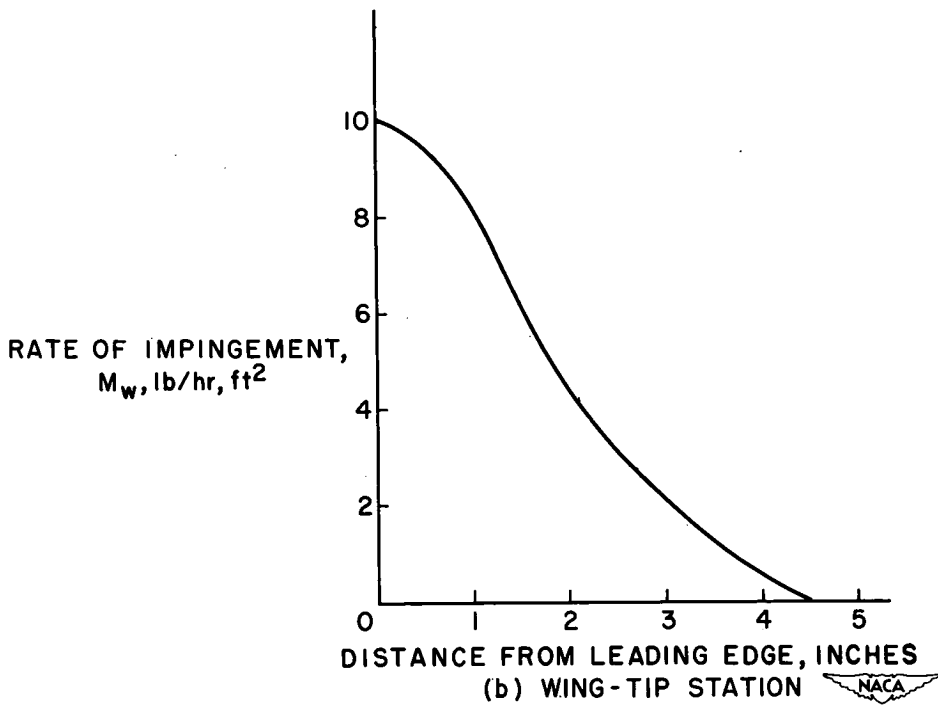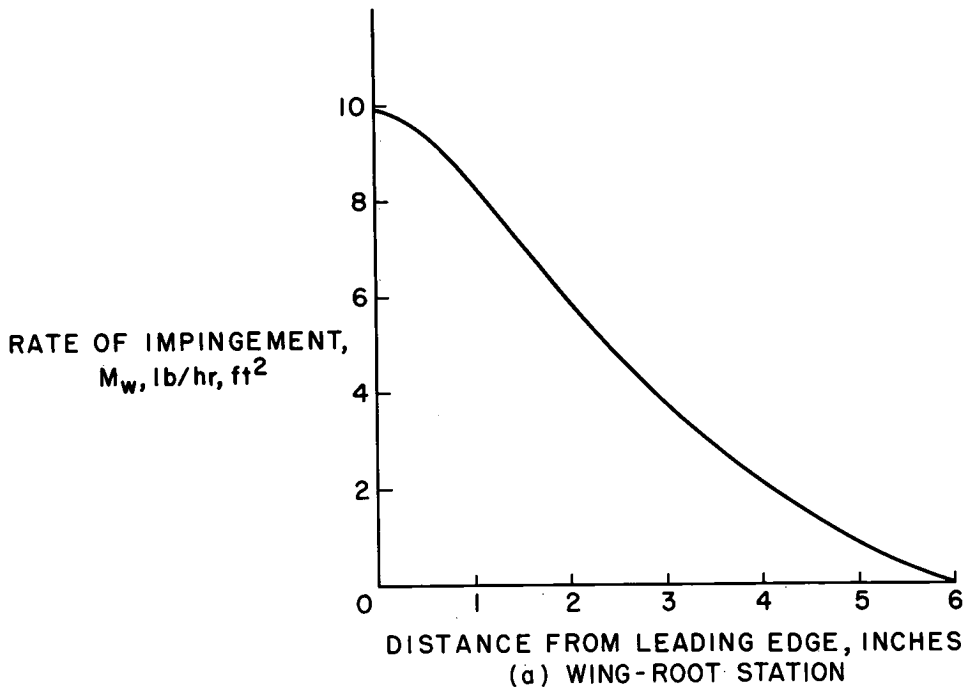
Figure 16.- Assumed distribution of rate of water impingement on wing upper surface.
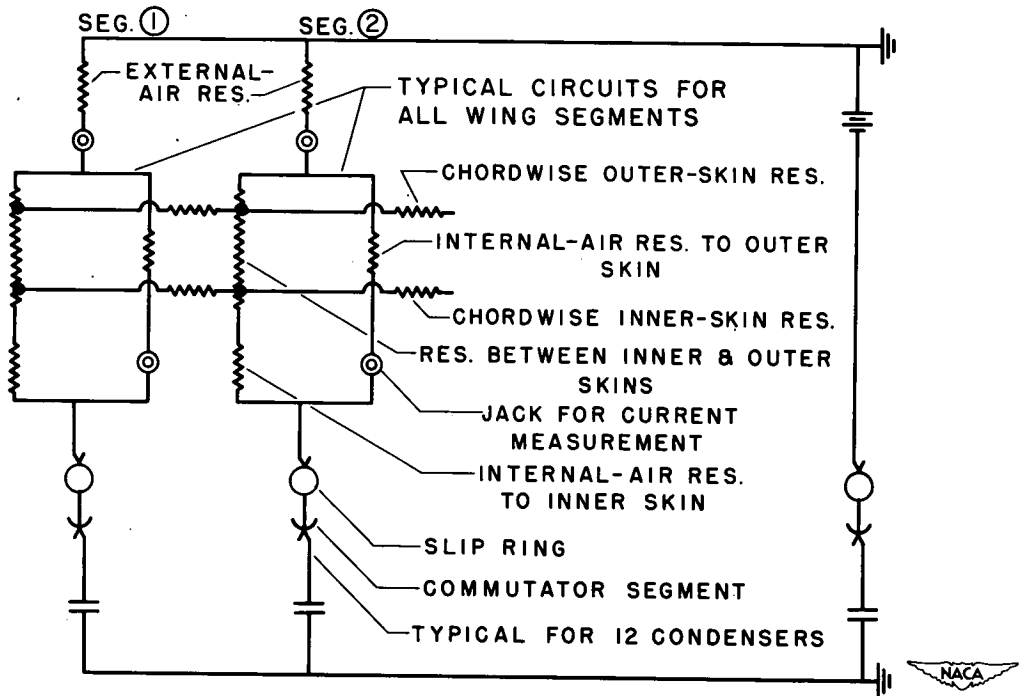
Figure 17.- Electrical circuit representing thermal circuit of an air-heated wing as used in application of electric model.
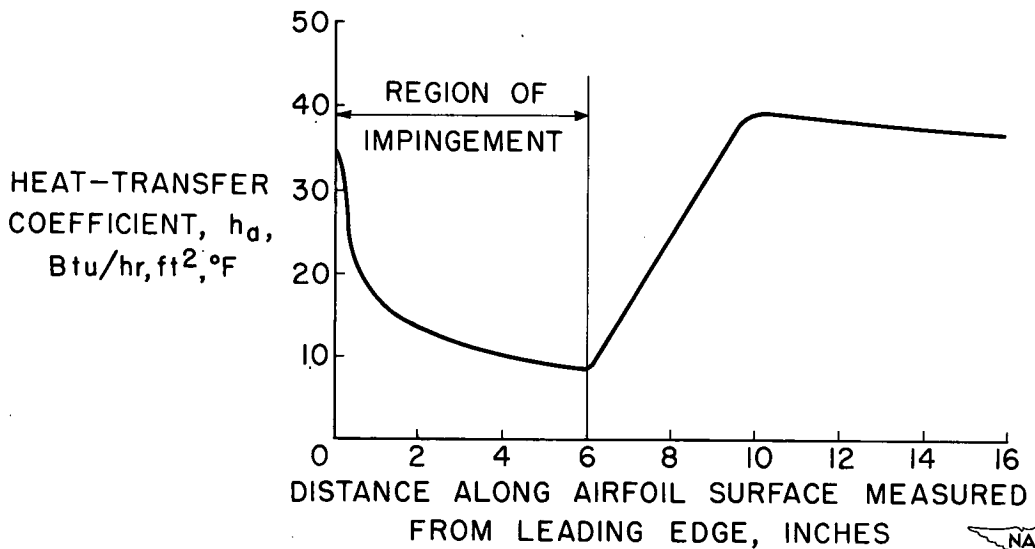
Figure 18.- Calculated variation of external convective heat-transfer coefficient along wing upper surface at root station.
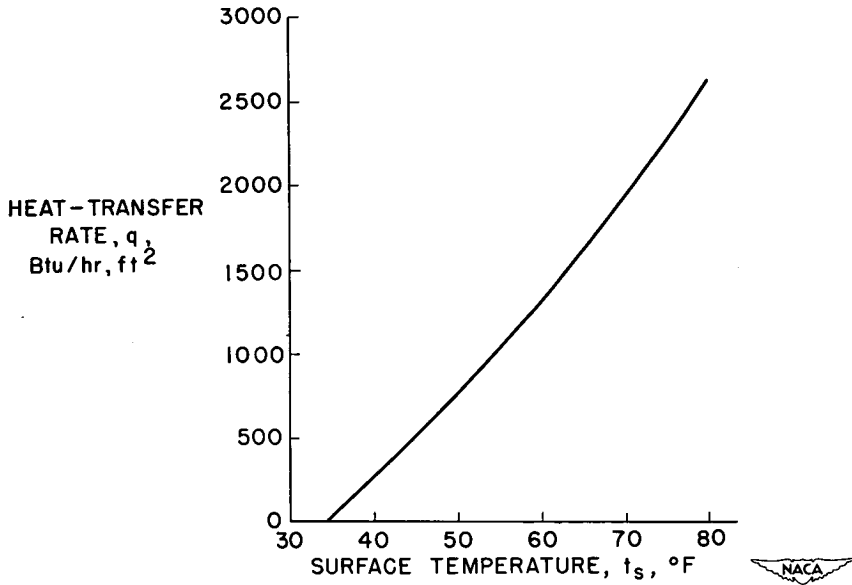
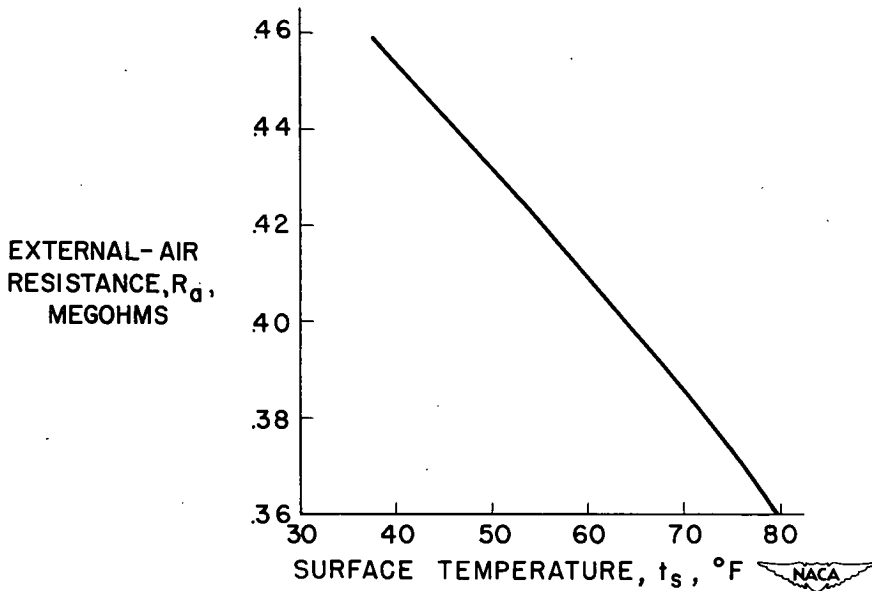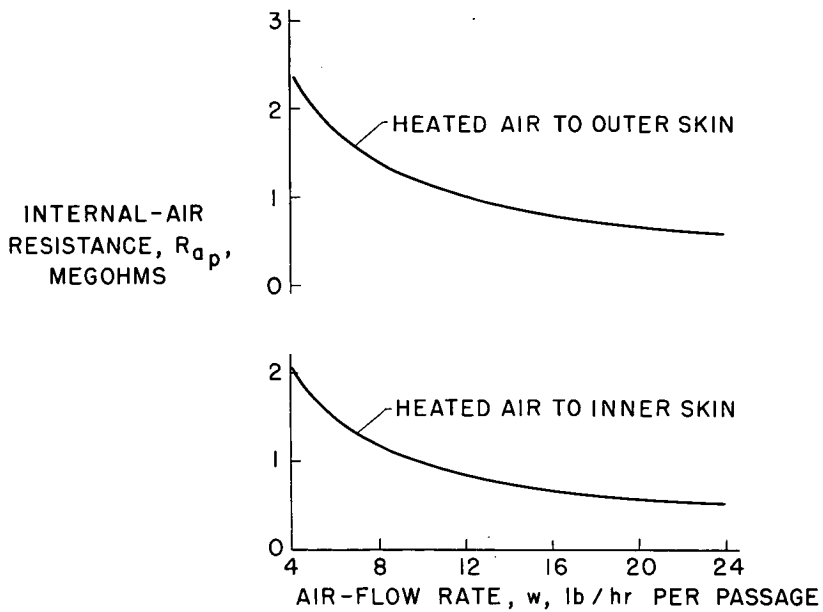Figure 19.- Heat-transfer rate as a function of surface temperature for segment 8 of wing surface at root station.

Figure 20.- External-air resistance as a function of surface temperature for segment 8 of wing surface at root station.

Figure 21.- Internal-air resistance as a function of heated-air-flow rate
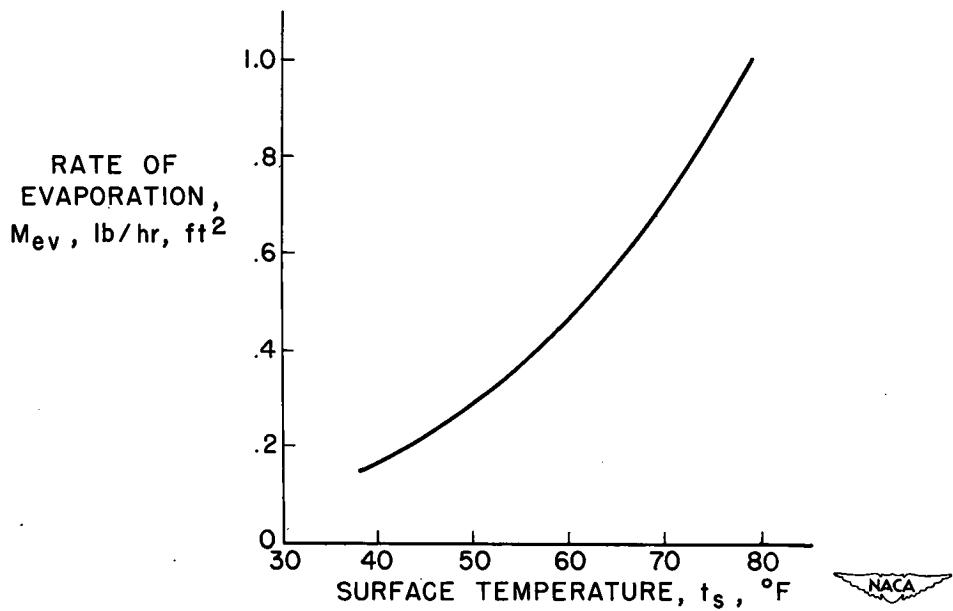for segment 8 of wing surface at root station.

Figure 22.- Evaporation rate as a function of surface temperature for
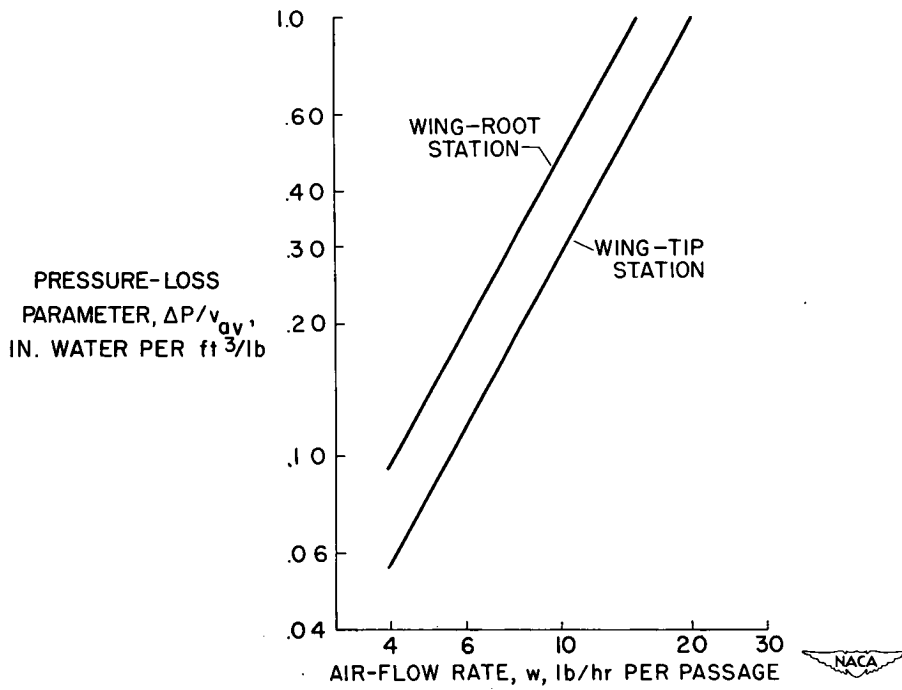segment 8 of wing surface at root station.

Figure 23.- Heated-air pressure-loss parameter as a function of air-flow rate through double-skin corrugations.